UNIVERSIDADE DE LISBOA
FACULDADE DE CIÊNCIAS
DEPARTAMENTO BIOLOGIA ANIMAL

Biological characterization of Rosette Stem Cells: a novel pluripotency state

Maria Madalena Cardoso Vaz dos Santos

Mestrado em Biologia Humana e Ambiente

Dissertação orientada por:
Prof. Dr. Derk ten Berge, Erasmus University Medical Center
Prof. Dra. Maria Gabriela Rodrigues, Faculdade de Ciências da Universidade de Lisboa

2021

Acknowledgments

Para a minha mãe e para o meu padrasto:

Obrigada por tudo. Por me ajudarem a cumprir este objetivo. Por todo o vosso esforço que me permitiu realizar este desejo de ir para fora e ter esta experiência única. Não o conseguiria ter feito sem o vosso apoio. Obrigada.

To my friends:

Lucas e Manuel, my support system through the – *very long* - writing phase. You were, and are, fundamental. Thank you.

Mafalda, for me, a part of Rotterdam will always be you. Thanks for making it feel more like home. I will always cherish this friendship, who cares about distance. The season is over, but not the show!

To Prof. Gabriela:

Thank you for all your care and availability, as well as for helping me clarify all my questions along this process.

To *The Lab*:

Irene, thank you for accepting the role of being my "supervisor". I can only imagine my frustration must have not been easy to handle sometimes. I will forever be grateful for our ability to bond over jamón, smoked meats and a twisted sense of humor.

Emiel, thank you for all – *quite a lot* – guidance that you gave me throughout the year, even though you didn't have to. I'm super grateful for all you have done, FOR REAL. My unofficial "supervisor".

LucaX, you brought me in into a world of imagination that made me feel much more comfortable in a new place, with new people. This was a big deal for me, thank you. Every Friday, in the back of my head, the Friday's afternoon playlist will be there.

Aggeliki (or, as I like to call you, Angelita), when I met you, you were the number one of my top 1 list of favorite Greek people. Today, it's a top 3, so you're struggling. Joking. You bring out the inner child in me. It's sometimes ridiculous, but I love it. Thank you for making it lighter, funnier and overall more bearable.

To Prof. Dr. Derk ten Berge:

Thank you so much for the guidance and the opportunity you gave me of working in your incredible group. It was an amazing, enriching experience that I will forever be grateful for.

Resumo

A pluripotência é definida como o potencial de gerar todas as linhagens celulares presentes no organismo adulto, com três estados distintos identificados. Recentemente descrito, o estado de pluripotência roseta é um estado reversível, intermédio entre os já estabelecidos estados *naïve* e *primed*, associados *in vitro* às células estaminais embrionárias (ESC) e células estaminais do epiblasto, respectivamente. *In vivo*, este estado intermédio associa-se às células do botão embrionário, na fase de peri-implantação do embrião, onde ocorre uma polarização e reorganização das células *naïve* numa roseta embrionária. As células estaminais roseta (RSC), já derivadas e sustentadas em culturas *in vitro* com recurso à inibição da sinalização Wingless-INT (Wnt) e proteína-quinase quinase ativada por mitógenos (MEK), têm o seu próprio perfil biológico. Uma das características especifícas das RSCs é a co-expressão do fator *naive* Klf4 e do fator *primed* Otx2.

Apesar do estado de pluripotência roseta estar já a ser caracterizado, ainda pouco se sabe relativamente à sua biologia. Com este estudo, o nosso foco assentou em aprofundar o conhecimento deste novo estado de pluripotência, através da caracterização das RSCs. Para isto, selecionámos processos biológicos que ocorrem, *in vivo*, no embrião na fase de pré-implantação. Nestes processos, comparando com a resposta das ESCs de *Mus musculus* sujeitas aos mesmos protocolos, testámos a resposta das RSCs de forma a observar se haveria uma alteração no seu potencial de desenvolvimento.

Um dos processos biológicos analisado foi a diferenciação de endoderme primitiva, uma das três linhagens celulares que se encontram no blastocisto de ratinho, tendo início no botão embrionário a E3.5. A capacidade das RSCs (e incapacidade das células estaminais do epiblasto) em derivar endoderme primitiva tinha já sido demonstrada em estudos prévios, através de diversos modelos *in vitro*. De modo a tornar a nossa abordagem mais robusta, utilizámos uma linha celular repórter Gata6::GFP, o primeiro marcador génico de endoderme primitiva a ser expresso. Adaptámos dois distintos e previamente publicados protocolos de diferenciação desta linhagem - a duas dimensões e através da formação de corpos embrióides - com recurso a fatores de indução. Os nossos resultados demonstraram que, quando submetidos ao processo de diferenciação, tanto as ESCs como as RSCs apresentam um aumento da expressão de marcadores génicos da endoderme primitiva. No entanto, o processo de diferenciação por formação de corpos embrióides revelou que no caso das RSCs, o marcador Gata6 é significativamente menos expresso. Este resultado sugere que a capacidade de diferenciação destas células em endoderme primitiva está comprometida, sendo significativamente menos eficiente.

O outro processo abordado, a diapausa embrionária, refere-se a um estado de dormência celular reversível no período de pré-implantação, que consiste na suspensão do crescimento embrionário. Este processo foi descrito em diversas espécies animais, incluíndo *Mus musculu*s, como uma estratégia para evitar condições desfavoráveis no momento do parto. *In vitro*, o processo descrito foi já mimetizado através da utilização de inibidores de Myc e mTOR. Estes permitem que as ESCs entrem num estado semelhante ao que ocorre *in vivo*, observando-se uma diminuição no *splicing*, na transcrição e síntese proteica. Simultaneamente, ocorre uma redução acentuada da proliferação e consequente dormência celular. Os nossos resultados, utilizando estes mesmos inibidores indutores de diapausa, revelaram uma diferença na resposta entre as ESCs e as RSCs. Foi observada uma supressão superior a nível da expansão celular nas RSCs, que aqui sugerimos dever-se a um aumento da morte celular destas quando induzidas em diapausa, mantendo, no entanto, o seu potencial pluripotente após recuperação deste processo. Com base nos resultados obtidos, sugerimos que as RSCs apresentam uma capacidade reduzida para entrar num estado de diapausa.

A acrescentar aos processos biológicos já mencionados, focámo-nos também num outro ponto essencial no desenvolvimento embrionário. As alterações metabólicas ao longo da progressão da pluripotência foram já descritas como fundamentais para a transição celular. No estado *naive*, as células apresetam um metabolismo misto com respiração mitocondrial e atividade glicolítica, passando para um metabolismo exclusivamente glicolítico no estado *primed.* Como tal, considerando os perfis metabólicos associados a distintos estados de pluripotência, analisámos os níveis de fosforilação oxidativa das RSCs, comparando com as ESCs. Os nossos resultados demonstraram diferenças entre os dois tipos celulares, apresentando as RSCs uma taxa de consumo de oxigénio geral mais baixa, que se traduz em níveis mais baixos de respiração mitocondrial. Esta tendência é também observada em células *primed* e está associada a um estado de pluripotência mais avançado.

Neste trabalho identificámos respostas distintas das RSCs, em comparação com as ESCs, ao nível de processos de desenvolvimento embrionário e ao nível do perfil metabólico destas células, reveladoras dos seus estados de pluripotência distintos. Com isto, pretendemos aprofundar a caracterização particular do estado de pluripotência roseta, de modo a acrescentar ao conhecimento presente referente ao contínuo da progressão da pluripotência.

Palavras-chave: células estaminais roseta, endoderme primitiva, diapausa, metabolismo celular

Abstract

Pluripotency is defined as the potential to form all cell lineages present in the adult organism, with three different stages identified., The rosette pluripotent stage is a novel reversible pluripotent state, intermediate between the naïve and primed stage. This stage is associated to developmental period of the peri-implantation epiblast - where the naïve cells polarize and rearrange in an embryonic rosette. Rosette stem cells, correspondent to this state *in vitro*, have their own individual biological profile, showing a characteristic co-expression of the naïve factor Klf4 and primed factor Otx2.

Little is known about the biological status of the rosette stage. With this study we focused providing a deeper biological knowledge and characterization of rosette stem cells, concretely through the comparison with the naïve stage embryonic stem cells. For this purpose, we selected biological processes in which the behavior of the naïve cells has previously been described and tested the response of rosette stem cells, to observe if there is a change in developmental potential.

Primitive endoderm differentiation is a process that starts developing *in vivo* in the inner cell mass of the blastocyst, at E3.5. Our data revealed a significant difference when comparing both cell types. The adaptation of two *in vitro* differentiation protocols revealed that while both cell types show an increase in the expression of primitive endoderm markers, in the case of rosette stem cells, Gata6 is less expressed. This suggests that the differentiation of these cells into primitive endoderm is significantly less efficient. We then assessed the ability of the cells to enter diapause, a dormant reversible state of the pre-implantation epiblast. The results revealed a difference between both cell types in the response to diapause-inducing inhibitors. Rosette stem cells showed a bigger suppression in cell expansion that we here suggest being caused by increased cell death, while retaining their pluripotent potential after recovery.

Furthermore, and considering the importance of the metabolic shift for pluripotency progression and the previously established distinct metabolic profiles for naïve and primed pluripotent cells, we analyzed the oxidative phosphorylation levels of rosette stem cells. We observed that, in comparison to embryonic stem cells, these cells possess an overall lower oxygen consumption rate that translates in lower levels of mitochondrial respiration. This trend is also observed in primed cells.

Our work indicated differences in, not only the response to developmental processes, but also in the metabolic profile between embryonic and rosette stem cells. With this, we aim to specify the particular characteristics of the novel rosette pluripotent state, improving our knowledge on the continuum that is pluripotency progression.

Keywords: rosette stem cell, primitive endoderm, diapause, cell metabolism

Contents

List of Figures, Lists and Formulas

List of Tables

List of abbreviations

CHIR - CHIR99021

COX – cytochrome C oxidase

CT – cycle threshold

EB – embryoid body

EpiLC – epiblast-like cell

EpiSC – epiblast stem cell

ESC – naïve embryonic stem cell

E "X" – embryonic day "X"

FCCP - carbonyl cyanide-4 (trifluoromethoxy)phenylhydrazone

FCS – fetal calf serum

FGF2 - Fibroblast Growth Factor 2

H3K27me3 - histone H3 lysine 27 trimethylation

H3K4me3 - histone H3 lysine 4 trimethylation

ICM – inner cell mass

imTOR - mTOR inhibitor

iMyc - Myc inhibitor

IWP2 - inhibitor of WNT production 2

MEK – mitogen-activated protein kinase kinase

miRNA – microRNA

OCR - oxygen consumption rate

OxPhos – oxidative phosphorylation

PD - PD325901

PFA – Paraformaldehyde

PGCLC – primordial germ cell-like cell

PrE – primitive endoderm

RSC – rosette stem cell

TE – trophectoderm

TGFβ - transforming growth factor beta

Wnt – Wingless-INT

XCI – inactivation of chromosome X

XEN – extra-embryonic endoderm

1. Introduction

1.1. Stem cell biology and embryonic development processes

1.1.1. Pluripotency progression

Pluripotency is defined as the potential to form all cell lineages present in the adult organism. It starts to manifest in the inner cell mass (ICM) of the mouse blastocyst (E3.5) with a small group of homogeneous cells, expanding to a few hundred cells at the gastrula-stage epiblast and it is fully extinguished by the onset of somitogenesis (E8.0), when the cells are fully committed to a lineage (Osorno, R., Tsakiridis, A., Wong, F., *et al*. 2012).

Different stages of pluripotency have been previously described. Associated with an early developmental phase (E3.5), the naïve stage is represented by embryonic stem cells (ESCs) in culture, derived from the ICM of the pre-implantation mouse blastocyst. At a later moment, after implantation occurs (E4.5), in the mouse post-implantation epiblast, the primed stage can be found (E5.5-E7.5), represented by epiblast stem cells (EpiSCs) (Tosolini, M., Jouneau, A. 2015).

Although showing slightly different characteristics, the epiblast-like cells (EpiLCs) are also considered primed pluripotent cells, which are derived *in vitro* from ESCs. Regarding the transcriptome of the cells, EpiSCs present a substantially different gene expression profile from the original epiblast cells, with a closer resemblance to the late-gastrula stage embryo (E7.5). On the other hand, EpiLCs show a transcriptome similar to an earlier developmental stage - the pre-gastrulation epiblast (E5.5-E6). Contrarily to EpiSCs, the transcriptome of EpiLCs gives them the ability to form PGCLCs, which is a characteristic of epiblasts E5.5-E6 (Wu, J., Belmonte, J. 2015; Kojima, Y., Tam, O., Tam, P. 2014). Therefore, EpiLCs allow for a good model to study the ICM to epiblast transition since they represent an earlier developmental timepoint than the former (Hayashi, K., Ohta, H., Kurimoto, K., Aramaki, S., et al. 2011).

In vitro, both cell types can be cultured and maintained, although they require different growth conditions. For ESCs, the use of the commonly called 2i condition – consisting on the WNT agonist CHIR99021 (CHIR) and the MEK inhibitor PD325901 (PD) - , together with the cytokine LIF, allows for the maintenance of the naïve state. This occurs due to the activation of Wnt signaling by CHIR - inhibiting negative regulator of the Wnt/B-catenin pathway GSK3 (Martello, G., Smith, A. 2014). Additionally, simultaneous inhibition of the MEK signaling pathway, through suppression of MEK, blocks further cell differentiation. In parallel, LIF will promote self-renewal, through activation of Stat3, which will cause the cells to be sustained in this pluripotent ground state (Smith, A. 2017).

For EpiSCs, a culture condition that contains Activin A and fibroblast growth factor 2 (FGF2) is used to maintain a primed pluripotency stage (Neagu, A., van Genderen, E., Escudero, I., *et al*. 2020). For EpiLCs, the same factors as for EpiSCs are used (FGF2 and Activin A), in addition to an inhibitor of WNT production 2 (IWP2). However, they cannot be maintained for long periods of time since they start to differentiate or die after three days in culture (Smith, A. 2017).

Representing different stages of pluripotency, naïve and primed cells present some defining key differences. Besides the capacity to derive PGCLCs - present in ESCs but not in EpiSCs-, naïve and

primed cells also differ in their chimera forming ability. While ESCs are capable of forming blastocyst stage chimeras, primed cells lack this ability due to their developmental asynchrony, which leads to a limited capacity to form early cell lineages (Brons, G., Smithers, L., Trotter, M., *et al*. 2007). However, when injected in a post-implantation epiblast, primed cells can form low-contribution chimeric embryos (Weinberger, L., Ayyash, M., Novershtern, N., *et al*. 2016).

Another key difference between naïve and primed cells concerns the X chromosome inactivation (XCI). XCI is a form of compensation that occurs in mammals to balance gene expression in female cells. In the early developmental 4 cell-stage embryo, the paternal X chromosome inherited by the female diploid mouse zygote is inactivated, being reactivated only in the subset of cells of the ICM that will form the epiblast - ESCs (Hassani, S., Totonchi1, M., Gourabi, H., *et al*. 2014). Later on, at E5.5, XCI is reinstated in the epiblast - EpiSCs (and EpiLCs *in vitro*), with the random inactivation of either the maternal or paternal chromosome X (Deuve, J., Avner, P. 2011).

Naïve and primed pluripotency is ascertained in cells with the expression of pluripotency markers. Sox2 and Oct4 are two essential core pluripotency transcription factors, present during all pluripotency development and not exclusively in a specific stage. These transcription factors present a dual role, being essential for naïve pluripotency - ESCs cannot self-renew and differentiate without them – but with their overexpression leading to cell differentiation, which requires the ESCs to keep Sox2 and Oct4 transcription levels in a narrow threshold. (Smith, A. 2017; Rizzino, A. 2013).

Alongside Sox2 and Oct4 there are other transcription factors, the so-called naïve markers: Klf4, Nanog, c-Myc and Tbx3. These genes are expressed in the mouse pre-implantation epiblast and in *in vitro* ESCs, with its downregulation occuring in the immediate post-implantation epiblast. Contrary to Sox2 and Oct4, ESCs can survive the deletion Klf4, Nanog, c-Myc and Tbx3, however, their self-renewal ability is heavily compromised (Martello, G., Smith, A. 2014). The maintenance of a naïve stage is therefore regulated by this network of interconnected factors and as such, its dissipation leads to the cells exiting it (Smith, A. 2017).

The loss of the naïve gene network starts to occur *in vivo* at the peri-implantation mouse embryo, while *in vitro* it occurs when the cells are removed from the 2i or any other naïve culture medium. One important factor described as working as a trigger for differentiation is FGF4, which is regulated by Oct4/Sox2, that leads to Erk activation. Simultaneously, the endogenous repressor Tcf3 – a target of Oct4 - limits the expression of naïve transcription factors (Yi, F., Pereira, L., Merril, B. 2009; Weinberger, L., Ayyash, M., Novershtern, N. *et al*. 2016).

As the expression of the naive markers starts to diminish, the expression of Oct4 and Sox2 is maintained, and primed markers start to be expressed. Immediately after the embryo implantation, Otx2 expression, regulated by Oct4, is increased. Otx2 will then drive the activation of enhancer regions required for Oct4 binding, which will be essential for the exit from the naïve state (Yang, S., Kalkan, T., Morissroe, C., *et al*. 2014).

Alongside with Otx2, other primed markers such as Oct6, Fgf5 and Dnmt3b start to be upregulated in the post-implantation epiblast, and are characteristic of EpiSCs (Kalkan, T., Olova, N., Roode, M. *et al*. 2017). These same markers are present in EpiLCs. However, as previously mentioned, there are some differences at the transcriptome level between these two cell types, such as the Nanog and Sox2 downregulation in EpiLCs, which is not observed in EpiSCs (Hayashi, K., Ohta, H., Kurimoto, K., Aramaki, S., et al. 2011).

Following these changes in the pluripotency gene expression network, there is a remodeling of the chromatin landscape. In a naïve state, cells present a more accessible chromatin landscape, with lower abundance of constitutive heterochromatin, general DNA hypomethylation, as well as bivalent histone H3 lysine 4 trimethylation (H3K4me3)/ histone H3 lysine 27 trimethylation (H3K27me3) chromatin domains, associated with gene activation and repression respectively (Tee, W., Reinberg, D. 2014). This allows for the cells to silence developmental genes while keeping them poised for activation upon initiation of specific differentiation programs further ahead (Bernstein, B., Mikkelsen, T., Xie, X., *et al*. 2006). In the primed state, increased methylation levels are observed, specifically of H3K27me3, related to the upregulated expression of Dnmt3 in the post-implantation epiblast. There is also a decrease of bivalent chromatin domains, consequence of the activation of genes associated with differentiation programs (Kalkan, T., Olova, N., Roode, M. *et al*. 2016; Takahashi, S., Kobavashi, S., Hiratani, I. 2018).

1.1.2. Rosette pluripotency stage

As established before, two stages of pluripotency have been previously described, naïve and primed. However, pluripotency progression is a continuum and as such, cannot be compartmentalized into isolated and disconnected stages. In agreement with this, research efforts have been made to better understand the transition between the naïve and primed stage. A formative pluripotency stage between naïve and primed had been previously mentioned in the literature, however it was only anticipated to be a transient state and it lacked definitive biological characterization (Smith, A. 2017).

Represented by rosette stem cells (RSCs), the rosette pluripotent stage was introduced as an intermediate stage between naïve and primed pluripotency that can be derived and maintained *in vitro* for multiple passages. This stage is associated with the developmental period of the peri-implantation epiblast - where the naïve cells polarize and rearrange in an embryonic rosette - at E5.0 (Neagu, A., van Genderen, E., Escudero, I., *et al*. 2020). As representatives of a distinct pluripotency stage, RSCs have their own individual biological profile, sharing however similarities with both naïve and primed cells – for example, the ability of RSCs, like ESCs, to form chimeras upon blastocyst injection and the presence of two active X chromosomes.

Regarding the arrangement of RSCs, some particularities can be seen. ESCs are characterized as rich in bivalent domains (H3K4me3/H3K27me3) with a potential for both gene repression and activation (Bernstein, B., Mikkelsen, T., Xie, X., *et al*. 2006) when in comparison to EpiLCs. However, RSCs show an even higher presence of bivalent marks in primed genes that will be required for the progression from rosette to primed pluripotency, instating a more permissive state for primed progression. Another difference is the specific format of pericentric heterochromatin, which is a form of constitutive heterochromatin but shows an accumulation of the facultative heterochromatin marker H3K27me3 in RSCs. The accumulation of this marker in constitutive heterochromatin is not observed in either ESCs or EpiLCs. This, alongside with the erasure of the constitutive markers H3K9me3 and H4K20me3, leads to what seems to be a specific rearrangement of the chromatin landscape in RSCs (Neagu, A., van Genderen, E., Escudero, I., *et al*. 2020).

The gene expression of RSCs reflects their unique profile in comparison to the previously known pluripotent stem cells. As aforementioned, one of the first genes to be expressed when exiting the naïve state is the primed marker Otx2. Its expression is critical, with both the knock-out or overexpression of Otx2 affecting the transition of cells to a rosette stage. Alongside Otx2, the expression

of the naïve marker Klf4 defines the genetic profile of RSCs, before the transition to a primed profile of Otx2 and Oct6 expression (Neagu, A., van Genderen, E., Escudero, I., *et al*. 2020).

Strongly interconnected with the gene expression, the activity of Wnt/β-catenin and MEK signaling pathways is of extreme importance, acting as regulators for pluripotency progression. In the naïve state, Wnt signaling allows for the maintenance of the naïve markers and represses Otx2. Once this signal is downregulated, *in vivo*, Otx2 expression is induced, which enables the transition from the naïve pre-implantation epiblast to the rosette stage peri-implantation epiblast. As such, to be cultured *in vitro*, RSCs require the WNT inhibitor, IWP2 (Figure 1.1) (Neagu, A., van Genderen, E., Escudero, I., *et al*. 2020).

The transition to a primed stage begins with the cells organizing in a rosette shape through a central aggregation of actin fibers. Through action of MEK signaling, cell polarization occurs followed by lumen formation, along with the expression of primed factors such as Oct6. For this reason, besides IWP2 and LIF, the use of MEK inhibitor PD is essential for the maintenance of the rosette stage *in vitro*, preventing the cells from progressing to a more advanced stage (Figure 1.1).

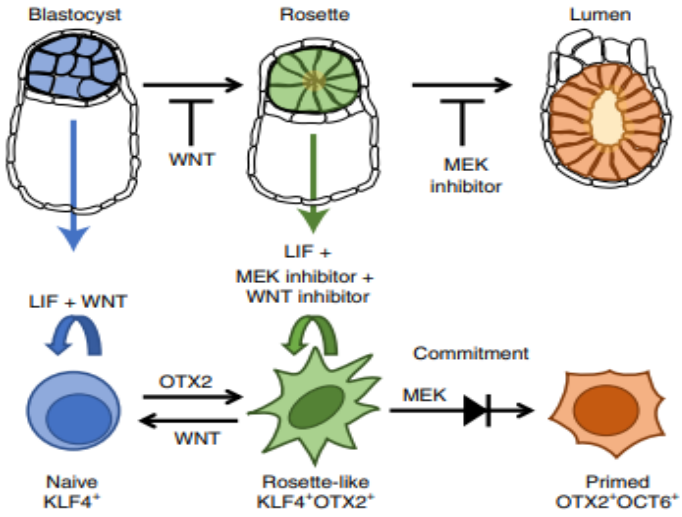

Figure 1.1 – **Representation of pluripotency progression from naïve to primed state**. Naive cells – capturing the ESCs present in the ICM of the blastocyst – are maintained by activation of Wnt signaling (through use of Wnt agonist CHIR) and LIF. When the Wnt signaling is down-regulated in vivo or inhibited *in vitro* with IWP2, the cells will exit the naïve stage, entering the rosette stage. Here, the expression of the naïve marker Klf4 is maintained, being induced the co-expression of Otx2. MEK signaling will lead to the commitment of these cells to a primed stage pluripotency and lumen formation *in vivo*, causing the expression of the primed factors such as Oct6, and continuing expression of Otx2. The combined use of LIF, IWP2 and the MEK inhibitor PD, will sustain the rosette stage cells *in vitro* (Neagu, A., van Genderen, E., Escudero, I., et al. 2020).

Overall, the Wnt and MEK signaling pathways regulate the rosette stage through two different points: the downregulation or inhibition of Wnt signaling that allows the cells to exit the naïve stage and the absence of MEK signaling that stops them from proceeding to primed pluripotency (Figure 1.1). It is important to mention that, when placed in a 2i condition, RSCs can convert back to ESCs, something that does not occur with primed cells since these are already committed to their cell fate, due to epigenetic barriers (Neagu, A., van Genderen, E., Escudero, I., *et al*. 2020).

By assessing RSCs transcriptome and comparing it with cells in the spectrum of differentiation from naïve to primed, it was shown that rosette stage cells resemble the transcriptome of 35h differentiating cells in primed conditions (FGF2+Activin A). Furthermore, when placed in primed differentiation media, RSCs switched considerably faster to a primed state in comparison with ESCs. This indicates that RSCs can transition directly to the primed stage while ESCs still need to go through the rosette stage (Neagu, A., van Genderen, E., Escudero, I., *et al*. 2020).

Overall, RSCs present characteristics that are more resemblant to naïve or primed cells or even a mixture of both, such as: the co-expression of naïve and primed factors; the X chromosome activation and the chimera forming ability; as well as distinct points like their chromatin landscape; and the ability to reconvert to a naïve pluripotency stage. With this, rosette stage pluripotency is established as a novel and unique intermediate pluripotency stage between naïve and primed (Neagu, A., van Genderen, E., Escudero, I., *et al*. 2020).

1.1.3. Primitive Endoderm differentiation

After fertilization, the mouse embryo cells start to divide transitioning from a 2-cell, to a 4-cell stage embryo, reaching a later 8-cell stage (E2.5). At this stage, increased adhesion occurs among the cells, known as blastomeres, in a process called compaction, where the cells acquire an apical-basal polarity. In the next couple divisions, cells divide in either a symmetric or asymmetric way, with the latter division generating a polar outer cell and an apolar inner cell. At this point, the blastocyst will have an inner and an outer layer, that will form the ICM and trophectoderm (TE), respectively (Hermitte, S., Chazaud, C. 2014).

When the embryo reaches the 64-cell stage (E3.5), the ICM cells start to exclusively express either Nanog or Gata6, in what is called the salt-and-pepper distribution. The expression of these genes defines the commitment of the cells to either an epiblast or primitive endoderm (PrE) lineage, respectively (Artus, J., Piliszek, A., *et al*. 2011). It is known that in the ICM, the epiblast progenitor cells express Fgf4 ligand – induced by Nanog. In PrE progenitor cells, the FGF receptor Fgfr2 is induced, making them more sensitive to Fgf4 induced signaling, which leads to the activation of the Fgf/MAPK signaling pathway, reinforcing the upregulation of Gata6 and a consequent repression of Nanog (Cho, L., Wamaitha, S., Tsai, I., *et al*. 2012; Schrode, N., Xenopoulos, P., Piliszek, A., *et al*. 2013). For this reason, Fgf4 has been described as an important regulator of PrE development.

At the late blastocyst stage (E4.5), the PrE and epiblast progenitor cells undergo spatial segregation. The PrE cells will migrate to the ICM surface in contact with the blastocyst cavity and form the PrE epithelial layer (Cai, K., Capo-Chichi, C., Rula, M., *et al*. 2008) (Figure 1.2). Continuing the developmental process, the primitive endoderm layer will give rise to the two other extra-embryonic endoderm layers: the visceral and parietal endoderm.

During the process that leads to the PrE epithelial layer formation, there is a complex gene network in action. At a first cell fate decision moment, the newly formed ICM and TE can be distinguished by their gene markers: Nanog, Gata6 and Oct4 in the ICM and Cdx2 in the TE (Figure 1.2). In the ICM, a second cell fate decision moment occurs, with the commitment of the cells to an epiblast or a primitive endoderm lineage (Hermitte, S., Chazaud, C. 2014).

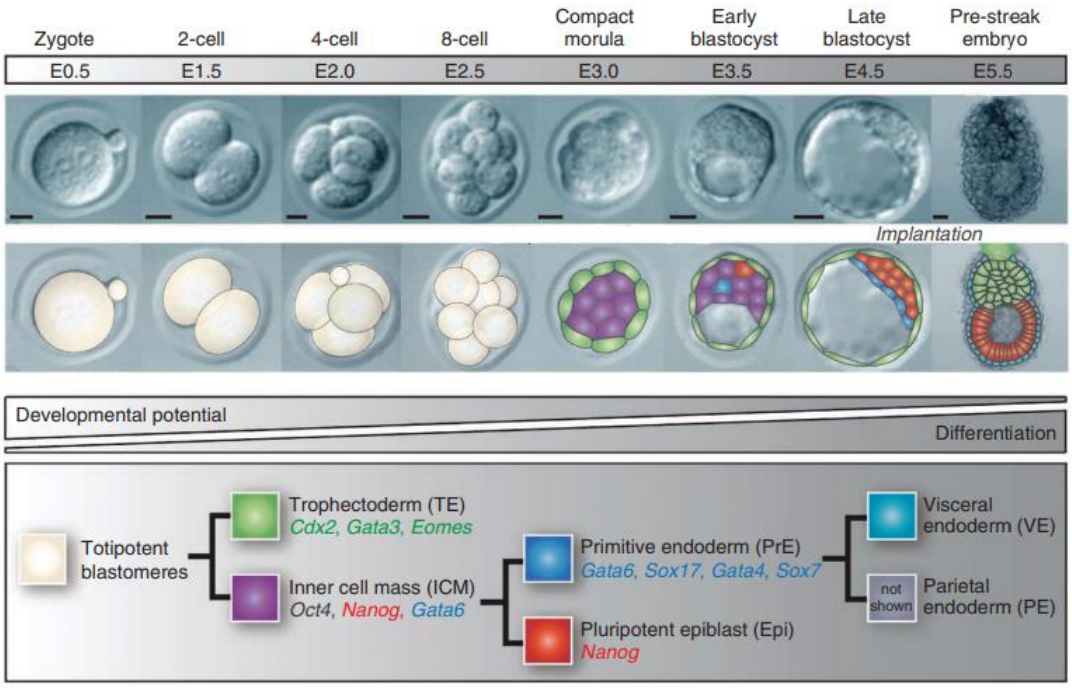

Figure 1.2 – **Mouse embryo developmental process from E0.5 until E5.5 regardng PrE cell fate decision moments**. The first segregating TE (TE cell markers: Cdx2, Gata3, Eomes) and ICM cells (ICM cell markers: Oct4, Nanog, Gata6). A second cell fate decision moment occurs with the commitment of cells to a PrE (PrE cell markers: Gata6, Sox17, Gata4, Sox7) or epiblast fate (epiblast cell markers: Nanog). The primitive endoderm layer will then give rise to the formation of visceral endoderm and parietal endoderm (Niakan, K., Schrode, N., Cho, L. *et al*. 2013).

As previously mentioned, two main markers are associated with the initial segregation of the progenitor cells: Nanog, expressed in the epiblast progenitor cells and Gata6, expressed in the PrE progenitor cells. However, in PrE cells, other markers are identified as having important roles in its development, with some expressed even before the migration that leads to the formation of the PrE epithelial layer. Sox17, Pgdfr-α and Gata4 are described in the literature as, alongside Gata6, markers for the primitive endoderm layer. Sox17 expression is detected as early as the 32-64 cell stage embryos, in a stage where a salt-and-pepper distribution is still effective. Noticeably, the expression of this gene occurs only in cells expressing Pdgfr- α, suggested to be the first PrE marker to be expressed after Gata6 (Plusa, B., Piliszek, A., Frankenberg, S., *et al*. 2008). Gata4 is expressed later on, at the 64-cell stage embryo, marking the moment where Nanog and Gata6 gene expression starts to be exclusive in the progenitor cells (Kang, M., Piliszek, A., Artus, J., *et al*. 2013).

The abovementioned genes present different roles in the PrE development process. Pdgfr-α is known to promote actin reorganization, directing cell movement but also integrin-induced enhancement of cell migration. In the case of Sox17, its role is not associated directly with PrE differentiation but instead with the maintenance of its epithelial integrity. For this reason, Sox17 null blastocysts present defects that lead to a premature differentiation and PrE cell migration along the TE. Expressed after Sox17, Gata4 is essential for the cell signaling required for the spatial segregation of the epiblast and PrE, with null embryos for this gene displaying severe defects in endoderm formation, dying as a result of it (Artus, J., Piliszek, A., Hadjantonakis, A. 2011; Cai, K., Capo-Chichi, C., Rula, M. *et al*. 2008).

In vitro, PrE or extra-embryonic endoderm (XEN) cells were successfully derived with the use of a low-dose of differentiation-promoting agents such as retinoic acid, the most potent natural form of

vitamin A. This agent binds to ligand-inducible transcription factors that will either activate or repress downstream gene expression (Soprano, D., Teets, B., Soprano, K. 2007). Activin is another agent used for this purpose, which activates the Nodal-signaling pathway. Nodal is a member of the transforming growth factor beta (TGFβ) family of growth factors, important for regulating embryogenesis and expressed in PrE (Cho, L,. Wamaitha, S., Tsai, I. *et al*. 2012.; Pauklin, S., Vallier, L. 2015).

XEN differentiation protocols tested both mESCs and EpiSCs, in a two dimension and embryoid body (EB) setup (Niakan, K., Schrode, N., Cho, L., *et al*. 2013; Cho, L,. Wamaitha, S., Tsai, I. *et al*. 2012; Vrij, E., Scholte op Reimer, Y., Frias Aldeguer, J., *et al*. 2019). For ESCs, the differentiated cells resembled XEN cells and showed expression of PrE gene markers such as Gata6, Sox17 and Gata4, as well as a similar morphology. In contrast, EpiSCs failed to derive XEN cells. This suggests that EpiSCs are unable to reverse their developmental commitment and that their differentiation potential might be restricted to germ layer lineages, aligning with their primed background (Cho, L,. Wamaitha, S., Tsai, I. *et al*. 2012).

To summarize, *in vivo*, cells start to acquire the gene expression profile characteristic of PrE cells in the ICM at around E3.5, with Gata6 expression, alongside other specific markers such as Pdgfr-α, Sox17 and Gata4. By E4.5, PrE and epiblast cells are spatially segregated, leading to the formation of the primitive endoderm epithelial layer. *In vitro*, these cells were successfully derived from ESCs, but failed to be derived from EpiSCs. This indicates that PrE potential is present in the pre-implantation epiblast and in naïve pluripotent cells, but absent from primed cells. However, it is unclear if RSCs possess PrE potential considering that, while representing an earlier developmental timepoint than primed cells, their more advanced timepoint in comparison to ESCs might still correspond to a restricted lineage potential.

1.1.4. Embryonic diapause

Embryonic diapause is a developmental process consisting of a pre-implantation period of embryonic growth arrest that occurs in the blastocyst stage. The development of the extraembryonic tissues and embryo is resumed when exiting this state, without any loss of developmental potential. This phenomenon has been described to occur in about 2% of mammalian species, including *Mus musculus*. It represents a way to avoid unfavorable conditions during birth, being triggered by external – such as harsh climatic conditions – and internal stimuli – metabolic stress caused by lactation (most common cause in *Mus musculus*) (Ptak, G., Tacconi, E., Czernik, M. *et al* 2012; Renfree, M., Fenelon, J. 2017).

In vivo, the mouse embryonic diapause is controlled by hormone regulation and can be mimicked with an ovariectomy, which stops the estradiol production needed for implantation. If the pregnant female is still lactating at E3.5, there is an increase in prolactin levels that prevent the estrogen surge, and the blastocyst enters the diapause state. While the blastocyst is in this dormant state, it stays in the uterine crypts, with no further implantation occurring (Fenelon, J., Banerjee, A., Murphy, B. 2014).

When entering diapause, the mouse blastocyst cells will undergo a decrease in splicing, transcription and protein synthesis. This is followed by a change to a mainly glycolytic metabolic system and proliferation arrest, which concludes in a dormant cellular state (Scognamiglio, R., Cabezas-Wallscheid, N., Thier, M.C. *et al.* 2016). Even though the mechanisms that regulate this process are still

not fully known, it was described that higher levels of microRNA (miRNA) in the diapause blastocyst will cause degradation of the transcripts. Consequently, mRNA will not be translated to proteins essential to continue the developmental process, which will result in a lower overall level of gene expression (Fenelon, J., Banerjee, A., Murphy, B. 2014). Let-7a is one of the known miRNAs present in these cells. Associated with targets that control cell proliferation, it was shown that when overexpressed in the mouse embryo, Let-7a prevents implantation and induces diapause (Liu, W., Cheng, R., Niu, Z., *et al*. 2020).

When exiting diapause, several cell processes are reactivated, leading to an increase of DNA, RNA and protein synthesis. This results in the upregulation of the cell metabolism to "pre-diapause" levels, the resumption of development and subsequent embryo implantation (Fenelon, J., Banerjee, A., Murphy, B. 2014). *In vitro*, studies have mimicked a diapause-like dormant state in ESCs with the use of Myc (iMyc) and mTOR (imTOR) inhibitors (Scognamiglio, R., Cabezas-Wallscheid, N., Thier, M.C. *et al.* 2016; Bulut-Karslioglu, A., Biechele, S., Jin, H., *et al*. 2016).

Myc, a transcription factor family comprising c-Myc, N-Myc and L-Myc, is an important regulator of cell proliferation and differentiation. Through regulation of RNA Polymerases I, II and III, Myc is involved in processes associated with myc-dependent gene transcription, cell growth, cell cycle control and metabolism (Hurlin, P. 2005). The importance of this transcription family factors was established when showed that, while L-Myc depleted embryos develop normally, c-Myc and N-Myc null embryos do not surpass E11.5. In these cases, the majority of defects is attributed to the incapacity to maintain sufficient levels of cell proliferation (Scognamiglio, R., Cabezas-Wallscheid, N., Thier, M.C. *et al.* 2016).

The understanding of the role of Myc in cell proliferation was strengthened by the observation of low levels of Myc in quiescent cell areas in the developing embryo. In these areas, there is a correlation of low levels of Myc to low levels of cell proliferation and an almost inexistent presence of c-Myc proteins and transcripts in diapaused embryos (Hurlin, P. 2005; Scognamiglio, R., Cabezas-Wallscheid, N., Thier, M.C. *et al.* 2016). As stated above, *in vitro* inhibition of Myc by either the use of a chemical inhibitor or by double knockout of c-Myc/N-Myc was shown to induce a diapause-like dormant state. When entering this state, the cells showed a downregulation of an extensive gene list, that includes categories such as metabolism, biosynthesis and cell proliferation. Simultaneously, there was an upregulation of gene categories associated with maintenance and cell survival. Importantly, when restoration of Myc levels occurred, the cells exited this quiescent state and resumed cell cycle alongside all translational activities. This established c/N-Myc activity as specifically important for cellular proliferation, but not essential for expression of naïve ground pluripotency markers that are continuously expressed during this diapause-like state (Scognamiglio, R., Cabezas-Wallscheid, N., Thier, M.C. *et al.* 2016).

Another pathway known to be able to induce mammalian embryonic diapause, mTOR – composed by mTOR complex 1 and mTOR complex 2 - is a key sensor for nutrient availability and a regulator for cell growth. Its deregulation is associated with diseases where growth is deregulated and homeostasis is compromised, namely cancer, metabolic diseases and ageing (Hussein, A., Wang, Y., Mathieu, J. *et al*. 2020).

It is known that the mTOR pathway is also involved in the process of starvation-induced diapause. This occurs through mTOR inhibition, caused the by high levels of glutamine associated with the high glycolytic metabolism in diapause. As a consequence, autophagy is induced, which enables a self-controlled cellular degradation that acts as a source of energy in periods of low extracellular

nutrients. Similar to Myc inhibition, the use of imTOR was shown to promote a paused, but reversible, cellular dormant state that retains expression of naïve pluripotency factors (Bulut-Karslioglu, A., Biechele, S., Jin, H. et al. 2016).

The studies showing the use of Myc and mTOR inhibitors as an *in vitro* method to induce a diapause-like state, all resort to the use of ESCs, in line with the fact that embryonic diapause occurs at the blastocyst stage E3.5. We speculate that the more advanced rosette pluripotent stage, will be unable to enter this dormant state.

1.1.5. Stem cells metabolic profile

In general, ATP is produced either by oxidative phosphorylation (OxPhos), also known as mitochondrial respiration, or glycolysis. Even though both systems produce ATP, they do it differently: OxPhos uses the mitochondrial Krebs cycle and other redox reactions that NADH. This will then be oxidated, leading to ATP production. Instead, glycolysis proceeds by catabolizing glucose molecules to produce pyruvate and ATP via substrate-level phosphorylation (Shyh-Chang, N., Ng, H. 2017).

Pluripotency progression brings a metabolic shift, with the ESCs presenting a bivalent metabolic system with both OxPhos and glycolytic activity, and the EpiSCs an exclusively glycolytic system. This metabolic change has to do both with the environment in which the cells are inserted but also with the specific needs of the cell. Initially, the blastocyst encounters an oxygen rich environment, which allows ESCs to produce energy through aerobic respiration, a more efficient ATP production method (Teslaa, T., Teitell, M. 2015). As the embryo develops and reaches the implantation and post implantation stage, there is a change to a more hypoxic environment, that leads to a switch in metabolism to glycolysis, the profile seen in primed cells. Glycolysis, although not as efficient, will produce ATP at a higher rate (Gatie, M., Kelly, G. 2018). Besides the environmental change, the need to maintain embryonic stability by reducing DNA and protein damage from reactive oxygen species was also indicated as a motive for this shift (Shyh-Chang, N., Ng, H. 2017; Zhou, W., Choi, M., Margineantu, D. *et al*. 2012).

Other than the metabolic profile itself, the mitochondria shape between ESCs and EpiSCs also diverges. Interestingly, the ESCs show more immature mitochondria with restrictive oxidative capacity and lower copies of mitochondrial DNA in comparison to EpiSCs. However, the mitochondria of EpiSCs are less active. This has to do with the lower expression of cytochrome C oxidase (COX) genes in primed cells, that acts as a limiting aspect in mitochondrial respiration, resulting in a consequently reduced mitochondrial activity (Zhou, W., Choi, M., Margineantu, D. *et al*. 2012).

Due to the novel status of the rosette stage, it would be of interest to characterize the metabolic profile of RSCs, since the change from a bivalent to an exclusively glycolytic metabolism is one of the major changes that occurs during pluripotency progression.

1.2. Objectives

As previously mentioned, the rosette stem cell stage, represented by RSCs, is a novel pluripotency stage that displays the transcriptome of the peri-implantation epiblast and is an intermediate between the extensively characterized naïve and primed stages. However, considering that RSCs were recently described and introduced to the scientific field, an extensive study of these cells is required to

obtain a more complete and inclusive biological profile, needed for the complete characterization of the rosette stage. Accordingly, the main goal of this study is to **obtain a more profound knowledge of the rosette stem cell pluripotency stage through the biological characterization of RSCs**.

To proceed to RSCs characterization, we focused on the analysis of their metabolism and their behavior in biological processes associated with early embryonic development, embryonic diapause and primitive endoderm differentiation. For both processes, the response of naïve and primed cells was described. This allows for a direct comparison between the specific developmental and metabolic responses between pluripotency stages. As such, the specific objectives of this study are to answer the following questions:

1. Is the more advanced pluripotent state of RSCs, in comparison to ESCs, a barrier for primitive endoderm differentiation *in vitro*?

2. Is the developmental timepoint of RSCs compatible with the ability to undergo a diapause-like state?

3. Does the mitochondrial respiratory activity of RSCs reflect the shift in metabolism associated to later, more advanced pluripotent states?

2. Materials and Methodology

2.1. Cell lines and culture conditions

For the purpose of this study, ESCs and RSCs were used from mouse cell lines IB10, R1 and CGR8. Both cell types were cultured, in N2B27 + LIF media (see supplements, Table 6.1) with the specific additives for each condition - CHIR99021 and PD325901 at 3μM and 1μM final concentration, respectively, for ESCs, and PD325901 and IWP2 at 1μM and 2μM final concentration, respectively, for RSCs – and incubated at 37°C and 5% CO_2 levels. Cell culture passaging was made using Trypsin-EDTA, and Soybean Trypsin inhibitor, added in 1:10 to the volume of added Trypsin-EDTA.

Specifically for the experimental protocols regarding primitive endoderm, ESCs and RSCs from a Gata6::GFP reporter cell line – expression of the green fluorescent protein is dependent on GATA6 expression - of a C57BL6 x 129Sv genetic background, kindly made available by A. Hadjantionakis, were used, having been maintained in the aforementioned conditions during pre-experimental periods (Freyer, L., Schröter, C., Saiz, N. *et al*. 2015).

2.2. Primitive endoderm derivation

As previously mentioned, ESCs and RSCs from a Gata6::GFP reporter cell line were used in all experiments referring to the RSCs primitive endoderm derivation potential study. For this, experimental protocols – 2D Primitive endoderm differentiation assay (referring to Niakan, K., Schrode, N., Cho, L., *et al*. 2013) and Embryoid bodies model for Primitive endoderm differentiation (referring to Vrij, E., Scholte op Reimer, Y., Frias Aldeguer, J., *et al*. 2019) – were adjusted and adopted from previously published studies that showed the successful differentiation of ESCs into cells displaying primitive endoderm characteristics or XEN cells.

2.2.1. 2D Primitive endoderm differentiation assay

The Niakan protocol for PrE differentiation presented several methods for differentiation. The one of our interest and adapted to our study conveyed a 2D cell culture setup with use of growth factors, more specifically retinoic acid and activin, as a way to establish XEN cells from initial ESCs in 2i culture conditions (Niakan, K., Schrode, N., Cho, L., *et al*. 2013).

EXPERIMENTAL METHODOLOGY

Cell culture media

Standard XEN medium
85% RPMI (catalog. R7638)
13% FCS
1% Glutamax

1% Penicillin/Strep
0.1mM B-mercapto ethanol

cXEN derivation medium
Standard XEN media + 0.01uM Retinoic Acid [1] + 10ng/mL activinA

[1] Retinoic acid is light sensitive, work in the dark.

Procedure

The cell seeding surfaces were coated with 0.1% Gelatin in PBS and Fetal Calf serum (FCS)[2] and incubated at 37ºC for one hour, after which the FCS was aspirated. After one hour, the cells were plated (ESC and RSC) at the wanted density[3] in the previously coated dishes, using 2mL of Standard XEN media per 6 well plate. The cells were platted for three timepoints: day 7, day 10, day 13, and at day 7, the cells were platted in duplicate.

24h after the initial plating, the media was changed to cXEN derivation media and, 48h after, the media was changed to Standard XEN media. In the continuance of the experiment, the cells were washed, and the media refreshed every 2 days, carefully, preventing cells from detaching.

At day 7, the cells were washed carefully with PBS to remove any debris. After, the cells from one of the duplicates were tripsinized by using Trypsin-EDTA and pipetting vigorously, and the number of live cells was counted[4]. Furthermore, at day 7, 10 and 13 of differentiation, all samples were imaged using a fluorescence microscope for GFP detection[5] and RNA was collected[6].

[2] In the original protocol, on top of the previously mentioned coating, mouse fibroblast cells (MEF feeder cells) were plated as a feeder layer, in which the cells used for differentiation were seeded. However, considering the ESCs and RSCs culture techniques established in the laboratory, the protocols used for this dissertation do not resort to MEFs.

[3]Considering the fluctuation of optimal cell density depending on the cell type/line used mentioned in the 2D Primitive endoderm differentiation assay, ESCs and RSCs were plated at three initial densities per collection day: 1E+04 cells per cm^2 (density used for ESCs in the original protocol), 2E+04 cells per cm^2 and 3E+04 cells per cm^2 . See Table 6.2 in supplements for number of cells seeded per density.

[4]Cell counting consisted in properly mixing 10 µL of cell suspension and 10 µL of trypan blue (accounts for dead cells), placing 10 µL of the solution in a hemocytometer and counting number of cells (live and dead) in an automated counter.

[5]Cells imaged in fluorescence microscope Olympus ix70, with 10x objective, using a green filter for GFP detection. All settings regarding image capture were maintained constant in-between experimental replicates.

[6] RNA extraction from cell samples proceeded following the RNeasy Mini Kit protocol from Qiagen (see supplements, Protocol A).

Notes: Attempts were made to passage XEN cells when they reached 90% confluency with both Trypsin (using Standard XEN media to neutralize it, as described in the original protocol) and TE however, due to high levels of cell death, the 13 days of differentiation occurred without passaging the cells. Optimization of this step is advised for further experiments.

Treatment and analysis of samples

The RNA treatment and DNase digestion from the collected samples at point 6 of the protocol were made following RNeasy Mini Kit instructions for "Protocol: Purification of total RNA from Animal Cells using Spin Technology" and "DNase Digestion with the RNAse-Free DNase Set" (see supplements, Protocol A).

Following the RNA treatment, the concentration of RNA in each sample was measured with a Nanodrop Spectrophotometer, using 1µL of each sample to do the measurements (in duplicates), initiating the readings with a blank measurement using RNase free water.

The levels of naïve pluripotency marker Nanog, PrE gene markers Sox17, Gata4 and Pdgfrα, and housekeeping gene Gapdh in the collected cell samples that underwent the differentiation protocol and controls (ESCs and RSCs in 2i and rosette media, respectively) were analyzed through qPCR. cDNA was synthesized from the treated RNA per sample[7], using the RevertAid First Strand cDNA Synthesis Kit (Thermofisher, see supplements Protocol B). Real-time PCR (qPCR) was performed on a C1000 Touch Thermal Cycler (Bio-Rad), using the iTaq Universal SYBR Green supermix (Bio-Rad, see supplements, Protocol C). Primer pairs for the target genes designed using BLAST software (see supplements, Table 6.3).

[7] All samples had a control for the cDNA synthesis protocol without Reverse Transcriptase (-RT), adding in those the same volume in RNase free-water.

qPCR running protocol cycle setup: (1) 95ºC for 5 minutes, (2) 95ºC for 30 seconds, (3) 55ºC for 30 seconds, (4) 72ºC for 1 minute, (5) Go to step (2) (39x), (6) 72ºC for 15 minutes, (7) Melt curve 65ºC to 95ºC, increment 0.5ºC for 5 minutes.

Visualization of qPCR results was made using the CFX Manager software. Gene expression measured values of target genes – Nanog, Sox17, Gata4, Pdgfrα – were normalized against the expression level of the housekeeping gene (Formula 2.1).

Target gene normalized expression= 2^[(CT Gapdh)-(CT target gene)]

Formula 2.1 – Normalized gene expression for the target gene by using its cycle threshold (CT) value and the CT from housekeeping gene Gapdh.

Experimental triplicates (independent assays) were considered for cell count and GFP imaging, while experimental duplicates were obtained for RNA collection and qPCR analysis.

2.2.2. Embryoid bodies model for Primitive endoderm differentiation

Other than the previously mentioned 2D Primitive endoderm differentiation protocol, the embryoid bodies model for Primitive endoderm differentiation, from the Rivron protocol, was adopted in this study with the purpose of assessing Primitive Endoderm formation in a more quantitative, controlled environment (Vrij, E., Scholte op Reimer, Y., Frias Aldeguer, J., *et al*. 2019). 96-wells-plates with non-adherent hydrogels with 430 microwells per well were used to allow cells aggregation and EB's formation. PrE differentiation was assessed by using the previously mentioned Gata6::GFP reporter cell line and defined growth media. Gata6 expression was quantified by counting the number of GFP expressing EBs in each specific well. To be noted that, while in the original Rivron Protocol the PrE marker initially used in the EBs is Pdgfrα, we used Gata6 due to reporter cell line availability.

EXPERIMENTAL METHODOLOGY

Cell culture media

Basal medium (B27N2)
1:1 DMEM/F-12 (containing sodium pyruvate + glutamine): Neurobasal media
0.5% N2 supplement
1% B27 supplement
0.5% Glutamax
10mM NEAA

mESC medium
DMEM/F-12 (containing sodium pyruvate + glutamine)
10% FCS
0.5% Glutamax
10mM NEAA

Conditional medium[8]
mESC medium
50uM B-mercaptoethanol
1% Pen/Strep
10nM Retinoic acid
10ng/mL LIF

Procedure

To start, the storage buffer (=PBS) was removed from the wells with microwells and replaced with 25 µL of basal medium per well and the plate was placed in the incubator to warm-up. After, ESCs were passaged to gain single cells and a suspension of 2.12E+05 cells/mL was prepared, of which were seeded 50 µL/well (7-12 cells per microwell). After the cells were seeded on top of the microwells, the plate was placed in the incubator for 15-20 minutes to allow the cells to settle in the microwells.

Conditional medium was prepared with the appropriate correction for the compounds[9]. Once the cells had settle in the center of the microwells, 150 µL of conditional medium/well were added and the plates were placed in the incubator. After 48h, 100 µL of the medium were refreshed with basal medium + 50 µM b-mercaptoethanol and 1% Pen/Strep.

72h after the initial plating, the EBs were counted using fluorescence microscope, after which the plate was placed back in incubator. At 96h, the EBs were counted[11] again and we proceeded with the Hoechst staining[10], to assess for live cells.

[8]Media that will constrain the cells' differentiation to PrE.

[9]Conditional media needs to have compound correction considering total volume per well (150 µL of conditional media per well with 5/3x correction - 25 µL for the hydrogel, 25 µL medium to increase seeding uniformity, 50 µL cell suspension and the 150 µL conditional medium)

[10]Hoechst staining (for live cells, 16.2mM solution): apply stain directly in the wells' media at 1:20000 (or make a dilution in PBS until final concentration of 1:20000) and incubate for 10 minutes at room temperature, in the dark. Live cells will stain blue.

[11] When counting, EB morphology (round or random) and GFP expression (criteria : one or more GFP expressing cells per EB lead to EB being counted as GFP positive) at both 72h and 96h was quantified, as well live cells (stained blue, Hoechst staining; criteria: one or more stained cells per EB lead to EB being counted as live). While EBs shape are typically of a rounded nature, for the purpose of this experiment, were counted as EB a cell aggregate contained in a microwell (Serup, P. 2017).

Note: In case of hydrogel damage and consequent decrease of number of intact microwells, were only counted the EBs that were inside a defined microwell.

Seven conditions were tested simultaneously in the PrE differentiation assay, one per well:

ESCs: Conditional medium (ESC)
Conditional medium without R.A (ESC -R.A)
Conditional media without LIF (ESC -LIF)
RSCs: Conditional medium (RSC)
Conditional medium without R.A (RSC -R.A)
Conditional medium without LIF (RSC -LIF)
Conditional medium (cells placed in 2i medium 48h before the experiment start : RSC 48h in 2i)

Experimental triplicates (independent assays) were produced.

2.3. Embryonic diapause

A diapause like-state has been mimicked in vivo, as previously mentioned, through the use of for Myc and mTOR chemical inhibition, with the cells entering a state of minimal or no cell division and restarting cell activity upon removal of the inhibitors (Scognamiglio, R., Cabezas-Wallscheid, N., Thier, M.C. *et al.* 2016; Bulut-Karslioglu, A., Biechele, S., Jin, H. *et al.* 2016). With the already established goal of understanding if RSCs could be capable of entering a diapause like state, cell number and

ability to form colonies of ESCs and RSCs cultures were assessed after a treatment using both of the aforementioned inhibitors.

EXPERIMENTAL METHODOLOGY

For the purpose of this experiment, iMyc (10058-F4, Calbiochem) and imTOR (mTOR1/2 inhibitor INK-128, MedChem) were used, at the published optimized final concentrations of 64μM and 200nM final concentrations, respectively (Scognamiglio, R., Cabezas-Wallscheid, N., Thier, M.C. *et al.* 2016; Bulut-Karslioglu, A., Biechele, S., Jin, H. *et al.* 2016). For the controls, was added the same volume of DMSO as the highest volume of inhibitor added.

Procedure

The cell seeding surfaces were coated with 0.1% Gelatin in PBS and Fetal Calf serum (FCS) and incubated at 37ºC for one hour, after which the FCS was aspirated. iMyc and imTOR inhibitor and the DMSO were added to the culture media and mixed by pipetting[12]. At 0h, ESCs and RSCs were seeded with the appropriate medium (2i or RSC media), according to their condition (control, with iMyc or with imTOR) [13].

After 24h, 24-well plates were coated with BME (1:100 in PBS)[14] and 0.1% Gelatin and, incubated at 37ºC for one hour, after which the BME was aspirated. The cells were washed gently with PBS, trypsinized and counted in all conditions. After, the cells were seeded at clonal density (400 cells/well for 24-well plate) in the BME coated plates for colony assays, with regular 2i media for all conditions (without inhibitors or DMSO).

72h after the cells were seeded at clonal density, the media was aspirated and 250 μL of 4% Paraformaldehyde (4% PFA) were added to each well, for 1-2 minutes. 4% PFA was then aspirated, and the cells were rinsed, gently, with a 1x rinse buffer (ex. TBST: 20Mm Tris buffered saline, 0.15M Sodium Chloride, 0.05% Tween-20). An Alkaline Phosphatase staining solution was prepared by mixing in a 2:1:1 proportion, respectively, the following reagents: Fast Red Violet, Naphtol AS-BI phosphatase solution and water[15]. 500 μL of the prepared mix were added to each well and the cells were incubated at room temperature, in the dark, for 15 minutes. After incubation, the total number of colonies per condition was counted, differentiating stained (undifferentiated, retain pluripotency) and not stained (differentiated, not pluripotent).

[12]Media should be warmed in water bath before adding iMyc, to prevent inhibitor crystallization.

[13] Number of cells seeded according to surface area of the well: 3E+05 and 1.2E+05 cells for a 6-well plate and a 12-well plate, respectively, in the case of ESCs, and 3.5E+05 and 1.6E+05 cells for a 6-well plate and a 12-well plate, respectively, in the case of RSCs. RSCs require a higher density to prosper in culture, data not shown.

[14]BME maintained in ice and handled with cold pipet tips.

[15]All reagents provided in Alkaline-phosphatase detection kit (SCR004, Millipore). This kit will stain for alkaline-phosphatase, a marker for undifferentiated pluripotent cells (Štefková, K., Procházková, J., Pacherník, J. 2015), determining which colonies remain undifferentiated.

Experimental triplicates (independent assays, two cell lines – R1, IB10 - per triplicate) were produced for cell counting at step 5. Experimental and biological replicates (one cell line per replicate - R1, IB10) were produced for colony assay.

2.4. Metabolic assay

To characterize RSCs in terms of their OxPhos pathway activity, a cell mitochondria stress test was performed, with the Agilent Seahorse XF24 Analyzer. This test measures the cells oxygen consumption rate (OCR), allowing for a direct quantification of mitochondrial respiration (Van Der Pluijm, I., Burger, J., Van Heijningen, P. *et al*. 2018).

The Seahorse metabolic assay experiments were made together with the department of Molecular Genetics of Erasmus Medical Center. Preparation of the samples and seeding of cells was performed in our department, while preparation of the assay components as compounds, media and cartridges (see supplements, Protocol D) was accomplished by the Molecular Genetics department.

Optimization trials were made for both cell number and carbonyl cyanide-4 (trifluoromethoxy)phenylhydrazone (FCCP) concentration before performing definitive assay.

The use of compounds will allow the measurement of OCR levels in the following sequence: the basal respiration is measured before the first injection, of oligomycin, which inhibits ATP synthase and will lead to a decrease in OCR related to ATP production; the second injection, of FCCP, causes a mitochondrial membrane potential disruption that leads to the maximal OCR level, allowing for measurement of spare respiratory capacity, through the difference of maximal and basal OCR; the third injection, of antimycin A, is applied for measurement of non-mitochondrial respiration, by inhibition of mitochondrial respiration (Agilent Technologies. 2019).

EXPERIMENTAL METHODOLOGY

For the metabolic assay, both RSCs and ESCs were analyzed, considering that the metabolic profile of the later is already know and will be helpful to analyze the results by comparing both cell types.

Procedure

First, the Seahorse XF24 cell culture microplate wells were coated with 0.1% Gelatin in PBS and FCS and incubated at 37ºC for one hour, after which FCS was aspirated. The cells to be analyzed were trypsinized- ESCs and RSCs - and a cell suspension was made (with standard media for each cell type: 2i medium to ESCs and rosette medium to RSCs) containing 1E+05 cells per 100 µL.

100 µL of the prepared cell suspension were placed per well, pipetting against the wall of the well. 5 wells were seeded (one line of the plate) per cell type to be tested. In the background wells (one per line), the same volume of total media was used as for the other wells, but no cells were seeded. The plates were then incubated at 37C/5%CO2, until cells were properly attached (~ 2h for ESCs/RSC). After the cells attached, 150 µL of standard

media for the specific cell type was added and the plate was incubated at 37C/5%CO2 overnight.

The day after the initial plating, the assay in the Seahorse XF24 analyzer was performed, following Agilent Seahorse XF Cell Mito Stress Test Kit User Guide instructions in sections "Day of Assay" (see supplements, Protocol D) (Agilent Technologies. 2019).

A gene set enrichment analysis was performed, resourcing to published RNA-Seq data referring to ESCs and RSCs - IB10, R1 and CGR8 cell lines - (Neagu, A., van Genderen, E., Escudero, I., *et al*. 2020) normalized with DESeq2 (Bioconductor package v3.10, RStudio v3.6.3), with GSEA v4.0.3 software from Broad Institute (1000 permutations; permutation type: gene set; metric for ranking genes: t-test). The gene set analyzed was composed by all *Mus musculus* genes present in the oxidative phosphorylation subsection, from the metabolic process group (biological processes) of the GOTree platform from MGI database.

The GSEA will show if the tested gene set genes are randomly distributed through our ranked data RNA-Seq list or are primarily represented in the top or bottom, which will tell us if the gene set is, if in any case, positively or negatively enriched (Subramanian, A., Tamayo, P., Mootha, V., *et al*. 2005).

2.5. Statistical analysis

All statistical analysis and graphic results were made using the IBM SPSS Statistics v26 software.

Required assumptions of data normality and homoscedasticity were tested using the Shapiro-Wilk and Levene's test (based on mean), respectively. According to the data characteristics and when the required data assumptions was fulfilled, the following parametric tests were applied: Student's t-test for two samples comparison and one-way ANOVA for multiple samples comparisons, followed by post-hoc Tukey's test. When the data required assumptions were not verified, non-parametric tests were used: U Mann-Whitney for two samples comparison with Bonferroni correction and Kruskal-Wallis test for multiple samples, followed by post-hoc Dunn's test.

3. Results and Discussion

3.1. Primitive Endoderm derivation

In order to assess the ability of ESCs and RSCs to derive PrE cells *in vitro*, both cell types were subjected to two distinct PrE differentiation protocols: a 2D cell monolayer protocol with use of growth factors activin and retinoic acid (Niakan, K., Schrode, N., Cho, L., *et al*. 2013) and a protocol based on embryoid bodies formation alongside with the use of retinoic acid (Vrij, E., Scholte op Reimer, Y., Frias Aldeguer, J., *et al*. 2019).

3.1.1. 2D Primitive endoderm differentiation leads to induction of tissue-specific markers

ESCs and RSCs subjected to the PrE differentiation protocol in different densities were counted at day 7 and imaged at day 7, 10 and 13 of differentiation for Gata6::GFP expression. RNA of the samples was then collected and analyzed for expression of PrE and pluripotency markers by qPCR. Gata6::GFP ESC and RSC cultures maintained with regular media (2i or rosette) were used as control. All camera settings were maintained between samples and timepoints (and replicates).

Initial cell density assessment of PrE differentiation

Optimal cell density is an important factor for PrE differentiation and it might differ between cell types due to, for example, different proliferation rates (Niakan, K., Schrode, N., Cho, L., *et al*. 2013). For that reason, at day 7 of differentiation, the cell number was counted to assess if certain cell densities resulted in a higher expansion of cells, and to establish the optimal density for both cell types. For both ESCs and RSCs, three densities were tested (see methodology, 2D Primitive endoderm differentiation assay): 1E+04, 2E+04 and 3E+04 cells per cm^2, and cell expansion calculated, translated by the cell number fold increase (see supplements, Table 6.4).

The results showed that at all densities, ESCs revealed a higher expansion than RSCs. RSCs showed a less expressive fold increase from the lowest to the highest cell density, a trend that was not observed for ESCs (Figure 3.1). We then proceeded to the statistical analysis of these results, to assess for significant differences in cell expansion between ESCs and RSCs and between the three densities tested.

First, both ESCs and RSCs were tested to see if there were any significant differences in cell expansion between densities. After testing and fulfilling the required assumptions of data normality and homoscedasticity (see supplements, Table 6.5), followed by a multiple comparison post-hoc Tukey test, one-way ANOVA showed significant differences between ESCs seeded at 2E+04 and 3E+04 cells per cm^2 and between RSCs seeded at 1E+04 and 2E+04 cells per cm^2, and 1E+04 and 3E+04 cells per cm^2 (see supplements, Table 6.6 and 6.7; Figure 3.1).

When comparing 2E+04 and 3E+04 cells per cm^2 densities, a positive correlation was found in ESCs between a higher cell seeding density and higher cell expansion. However, in RSCs we observed that the lowest density showed a significantly higher cell expansion compared to the others.

Overall, we could not associate one density with the highest cell expansion values for both cell types. While the lowest density could be seen as the preferred one – having the highest and second highest cell expansion for ESCs and RSCs, respectively - we had difficulties collecting enough RNA for analysis from this cell density. Therefore, we continued the PrE differentiation assays with all three densities.

Secondly, ESCs and RSCs were tested to observe if there was a difference between these cell types regarding cell expansion when submitted to the PrE differentiation protocol. After testing and fulfilling the required assumptions of data normality and homoscedasticity (see supplements, Table 6.5), t-test showed significant differences in cell expansion between cell types, in all the densities tested (p-value < 0.05) (see supplements, Table 6.8; Figure 3.1). These results indicate that when initially subjected to the PrE differentiation protocol, RSCs expansion occurs significantly slower than ESCs.

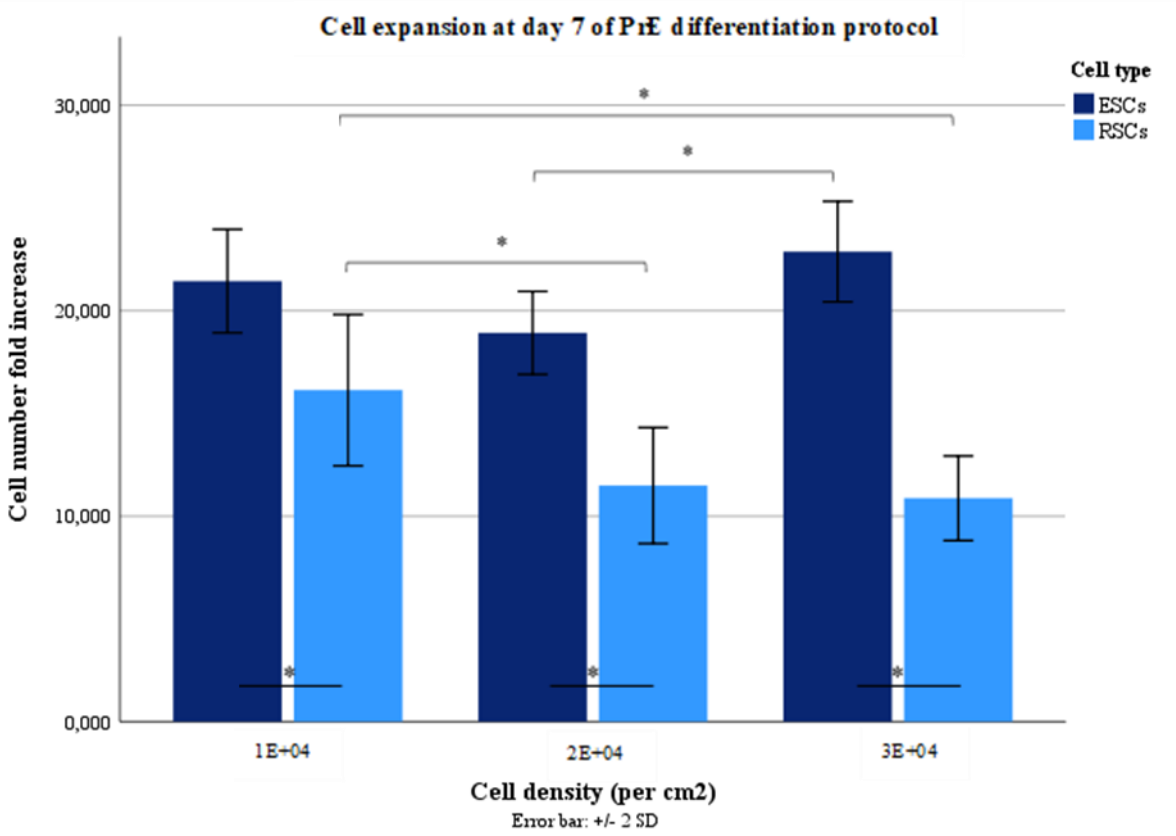

Figure 3.1 – **2D Primitive endoderm differentiation assay samples' cell expansion,** represented by cell number fold increase, **(Table 6.4) (number of live cells at day 7/ initial number of cells seeded) for both ESCs and RSCs**. Three initial seeding densities: 1E+04 cells per cm^2, 2E+04 cells per cm^2 and 3E+04 cells per cm^2. Based on mean values of all replicates. Standard deviation represented by error bar. *statistical analysis shows significant difference, with p-value < 0.05 (Table 6.6, 6.7 and 6.8).

Several factors could have interfered with the higher cell expansion observed in ESCs, such as a difference in the cell plating efficiency – although in each replicate both cell types were plated side-by-side. A difference in proliferation rate was also described, with RSCs proliferating slightly slower than ESCs (Neagu, A., van Genderen, E., Escudero, I., *et al*. 2020). However, the different cell expansion could also result from increased cell death for RSCs, due to a lower efficiency of differentiation to PrE.

Gata6::GFP expression imaging at day 7, 10 and 13 of differentiation

We first assessed the induction of Gata6-GFP as a marker for PrE differentiation (Plusa, B., Piliszek, A., Frankenberg, S., *et al*. 2008). ESCs and RSCs derived from a Gata6::GFP reporter cell line underwent the 2D PrE differentiation protocol for 13 days and were observed with a fluorescence microscope at days 7, 10 and 13. Both ESCs and RSCs presented GFP positive colonies in all samples, at each timepoint, and a clear difference in GFP expression levels was not detected (Figure 3.2). As expected, samples with a higher initial cell seeding density presented, at naked eye, more colonies (not shown).

Overall, the GFP expression was very heterogeneously distributed between colonies, in all samples from both cell types. An increase in GFP expressing colonies was observed -not quantified- at day 10 and 13, in comparison with the samples from day 7 (Figure 3.2 E, F, G and H).

At day 13, while the majority of cell colonies were GFP positive, the cultures contained some debris caused by cell death and a very high confluency level. Consequently, some colonies detached, likely due to overpopulation. As mentioned in the methodology section, passaging the cells at 90% confluency would be highly advised to improve analysis at day 13 or even more advanced timepoints in the PrE differentiation protocol.

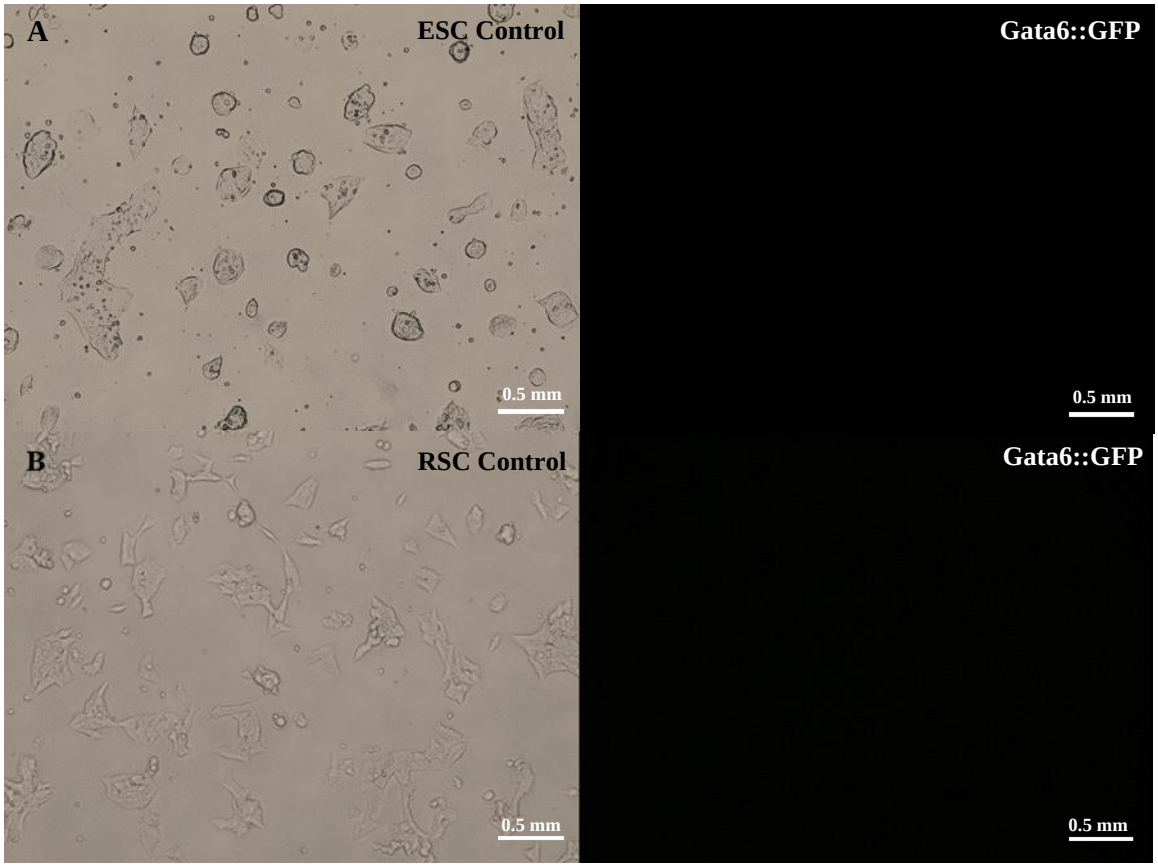

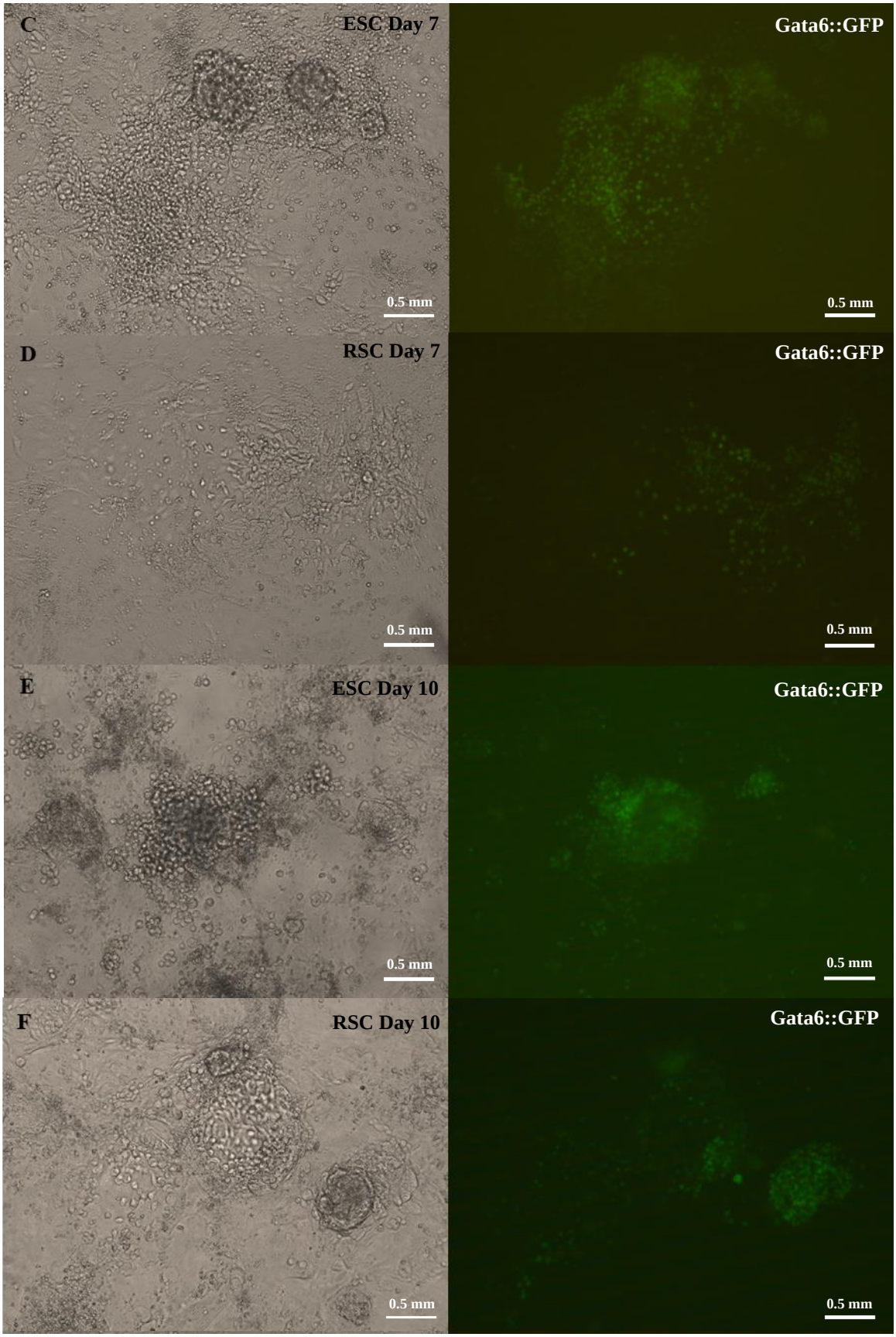
C
ESC Day 7
0.5 mm
Gata6::GFP
0.5 mm
D
RSC Day 7
0.5 mm
Gata6::GFP
0.5 mm
E
ESC Day 10
0.5 mm
Gata6::GFP
0.5 mm
F
RSC Day 10
0.5 mm
Gata6::GFP
0.5 mm

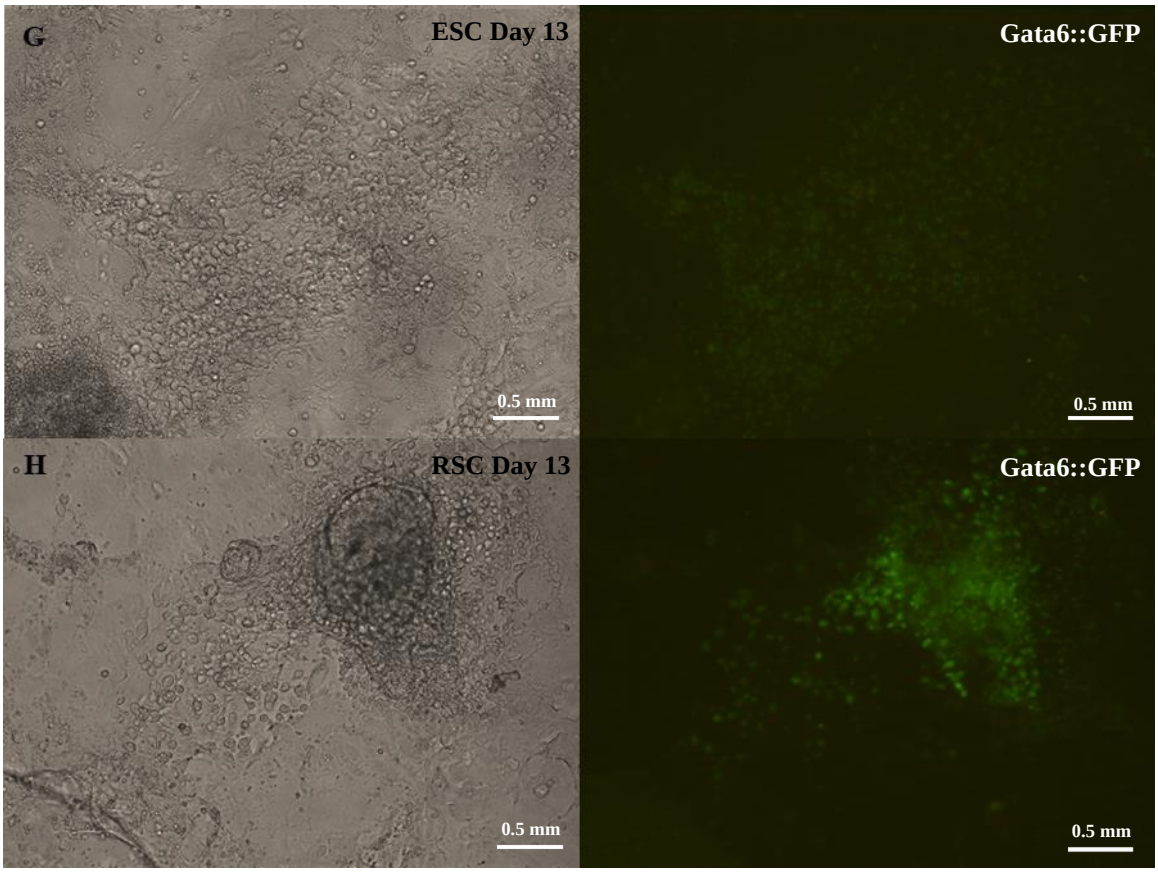

Figure 3.2 – **Gata6::GFP cell cultures under 2D Primitive endoderm differentiation assay and controls in standard culture media** (ESCs in 2i and RSCs in rosette medium). Pictures with fluorescence microscope Olympus ix70: ESCs (A) and RSCs (B) controls and samples derived from ESCs and RSCs Gata6::GFP reporter cell line at day 7 (C and D, respectively), day 10 (E and F, respectively) and day 13 (G and H, respectively). All pictures are from "2E+04 cells per cm^2" density.

The results revealed that both ESCs (as shown in Niakan, K., Schrode, N., Cho, L., *et al*. 2013) and RSCs express the primitive endoderm marker Gata6 when placed in a PrE inducing media. Nonetheless, it was not clear an association between a higher or lower Gata6::GFP expression level and a specific cell type or density.

To check if the cells that underwent the differentiation protocol acquired a PrE gene expression profile, RNA samples were collected and quantified for expression levels of other primitive endoderm markers such as Sox17, Gata4 and Pdgfrα, as well as for the naïve pluripotency marker Nanog. Simultaneously, RNA was collected from ESCs (in 2i media) and RSCs (in rosette media) from the Gata6::GFP reporter cell line (called day 0), to use as controls. Some samples containing insufficient RNA were excluded from qPCR analysis (see supplements, Table 6.9).

Real-time PCR results, after normalization against the housekeeping gene (see supplements, Table 6.10), were normalized against the day 0 expression values of target genes in ESCs or RSCs. This normalized gene expression reflects the number of times the gene level is superior or inferior in comparison to day 0 (Figure 3.3).

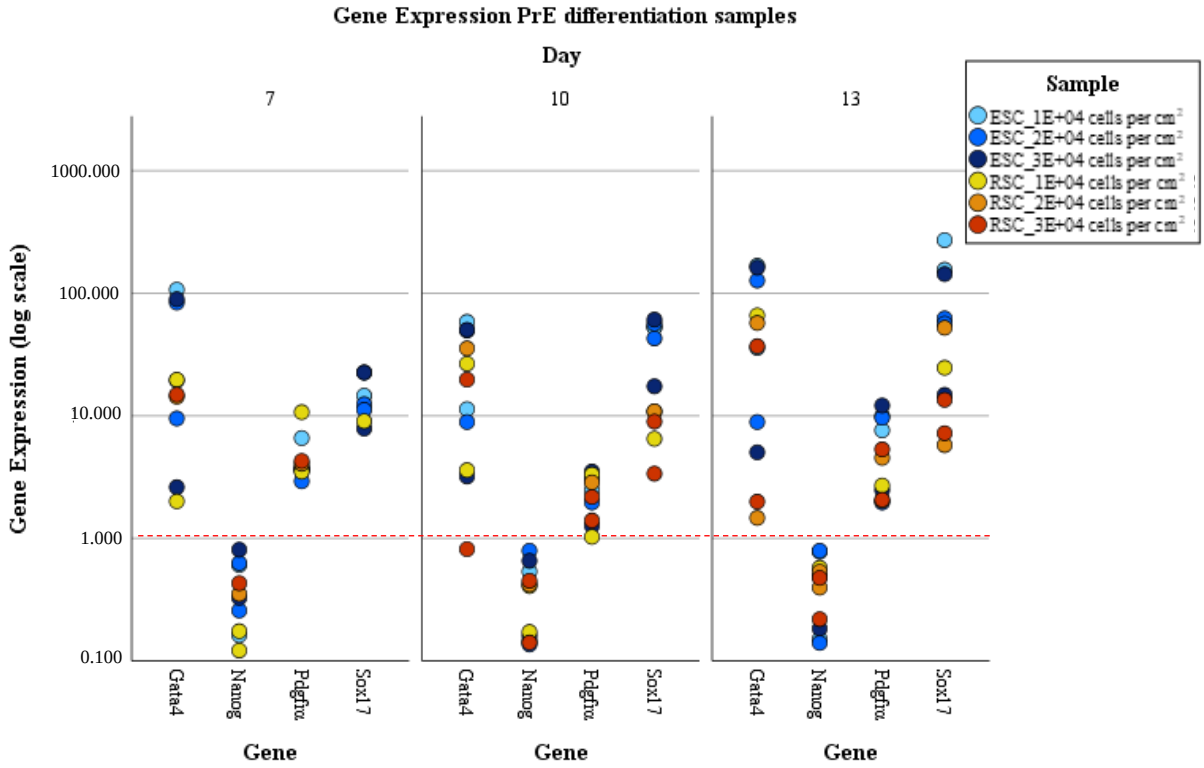

Figure 3.3 - **2D Primitive endoderm differentiation assay samples' gene expression ratio against day 0 (gene expression day X / gene expression day 0) for primitive endoderm markers Sox17, Gata4, Pdgfrα and naïve pluripotency marker Nanog**. Discrimination of all samples by initial cell seeding density and timepoint (day 7, 10 and 13). Values for both replicates (A and B) presented. Plotted values of Table 6.11. Markers above or below log scale 1 in Y axis represent a gene expression that is superior or inferior, respectively, comparing to the correspondent day 0 samples.

The results showed that both the ESCs and RSCs that underwent the PrE differentiation protocol presented, in general, a higher expression of PrE markers Sox17, Gata4 and Pdgfrα, and a lower expression of the naïve pluripotency marker Nanog in all timepoints, with the expression levels of these markers fluctuating between samples.

In several day 7 samples, Sox17 levels were not detected in the qPCR analysis (see supplements, Table 6.10). Considering that the primer pairs were tested for amplification of the right product, this suggests that the gene was not expressed in these samples (Figure 3.3).

The fluctuation of expression levels between experiments did not allow for a quantitative interpretation of the data (see supplements, Table 6.11). Several variables could be related to this, such as the reactivity levels of the differentiation inducing factors or the lack of homogeneous expression of these PrE and naïve pluripotency markers in XEN cells, previously described, which could suggest a heterogeneity in XEN cells population (Niakan, K., Schrode, N., Cho, L., *et al*. 2013).

According to the PrE differentiation protocol adapted for this experiment, a XEN cell line can take up to 20 days to be established (Niakan, K., Schrode, N., Cho, L., *et al*. 2013). As the more advanced timepoint collected was at day 13, it could be that the cells did not had enough time to undergo the full differentiation process, which could explain the undetected expression values of Sox17. In any case,

while in a preliminary stage, the Gata6::GFP expression together with the qPCR results indicate that, when exposed to PrE differentiation factors, both ESCs and RSCs start to express a gene profile with characteristics of that of cell committed to the primitive endoderm lineage (Cho, L., Wamaitha, S., Tsai, I., *et al*. 2012; Schrode, N., Xenopoulos, P., Piliszek, A., *et al*. 2013).

3.1.2. Primitive endoderm differentiation by RSCs in embryoid bodies is compromised

The ability of ESCs and RSCs to undergo PrE differentiation was also tested through a quantitative approach, using a protocol in which cells form embryoid bodies (EBs) in hydrogel microwells (Vrij, E., Scholte op Reimer, Y., Frias Aldeguer, J., *et al*. 2019). After the initial ESCs and RSCs Gata6::GFP reporter cell line seeding, all conditions were counted at 72h and 96h in several categories.

Gata6::GFP expression was used as the indicator of PrE differentiation and the number of GFP positive EBs was counted. A category was established to count the total of round EBs, characteristic that can be associated with the EB integrity (Brickman, J., Serup, P. 2017). To observe if there was any association between the EB morphology and the ability to express Gata6, a category was created that considered the percentage of round EBs, from the total of GFP expressing EBs. Furthermore, the number of live EBs at 96h was also counted.

For both ESCs and RSCs, a condition with all the components of the conditional medium (standard) and two others were tested. The condition without retinoic acid (R.A), known to be an inducing factor for PrE differentiation, tested if the absence of this PrE inducing factor would stop the differentiation of the cells. The condition without LIF, a cytokine responsible for promoting the pluripotent cells self-renewal, tested if, in the absence of it, a lower cell death rate would be observed. If verified, this could suggest that by lifting the restraint of pluripotent self-renewal imposed by LIF, the cells not able to follow the PrE lineage would be apt to differentiate into other paths (Niakan, K., Schrode, N., Cho, L., *et al*. 2013; Cho, L,. Wamaitha, S., Tsai, I. *et al*. 2012; Smith, A. 2017).

An extra condition was included for RSCs, to assess for possible epigenetic barriers present that could impact the ability of the cells to differentiate into PrE, after reverted to a naïve state (Neagu, A., van Genderen, E., Escudero, I., *et al*. 2020). For this, RSCs were maintained in 2i medium in the 48h previous to the experiment and then placed, in the beginning of the assay, in conditional medium with all the components.

The results are shown in Table 6.12, 6.13 and 6.14. Considering no significant differences were observed between the two timepoints regarding Gata6::GFP expression (see supplements, Table 6.15, 6.16, 6.17), the data analysis proceeded using the 96h collected results, converted to percentual values (Table 3.1).

To assess if ESCs and RSCs presented differences in EB formation or Gata6 expression ability, both cell types standard conditions were compared (Figure 3.4). We proceeded with either a student's t-test or a U Mann-Whitney test, after testing for the required assumptions of data normality and homoscedasticity (see supplements, Table 6.18). The results showed that ESCs, in comparison to RSCs, presented a higher proportion of round shaped, live and Gata6 expressing EBs. In addition, ESCs presented a higher proportion of round shape EBs from the total of those that expressed Gata6 (Table 3.1, 3.2).

In both cell types, all conditions that presented GFP positive EBs, revealed that an extremely high percentage of those were also round shaped (Table 3.1, Figure 3.5). This could indicate that the formation of an EB with a round morphology - that can be associated with its integrity (Brickman, J., Serup, P. 2017) - might be a stepping stone before the cells start to differentiate and express the PrE marker, Gata6.

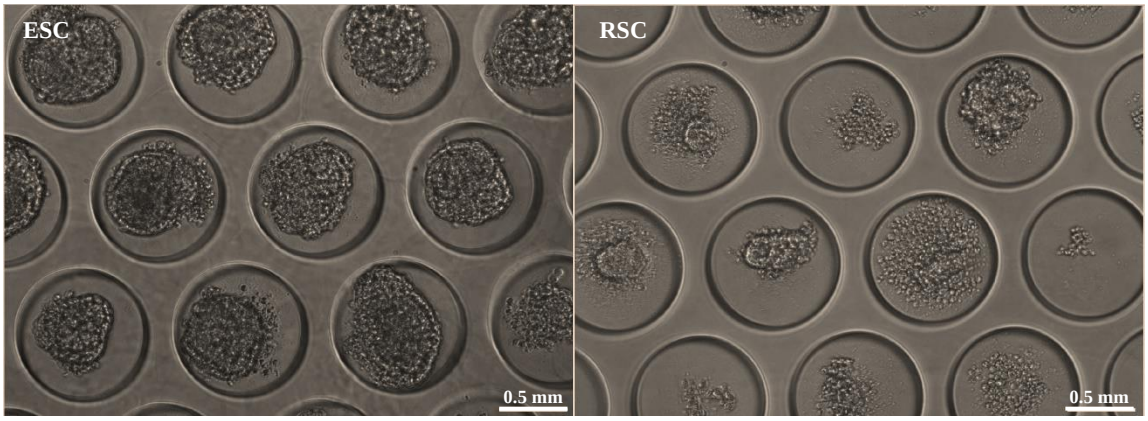

Figure 3.4 – **Embryoid bodies at 96h formed in ESC** (left) **and RSC** (right) **standard conditions of the embryoid bodies model for Primitive endoderm differentiation essay.** Pictures with Olympus ix70 microscope, 10x objective. Image scale 0.5mm

The embryoid body is characterized as an embryonic stem cell 3D structure. This, together with the significant lower proportion of EBs with round morphology observed in the RSCs standard condition, in comparison with ESCs, could lead to question the ability of these cells to form EBs (Table 3.2, Figure 3.5) (Niakan, K., Schrode, N., Cho, L., *et al*. 2013; Brickman, J., Serup, P. 2017). Associating this with the suggestion that the formation of a round shaped EB could act as a stepping stone, might explain the significantly lower Gata6 expression observe d in RSCs, when comparing to ESCs. However, in absence of RA, RSCs form a significantly higher proportion of round shape EBs (Table 3.1, 3.2). This indicates that their decreased EB forming ability in the standard condition is a consequence of the PrE differentiation induction and not an incapability of RSCs to form this structure.

While it is not completely understood why, when undergoing the PrE differentiation process, a difference in the EB morphology is observed between ESCs and RSCs. This could be explained by the higher cell death rate observed in RSCs (Table 3.1, 3.2), which might cause dead cells to form clumps that would be quantified as a random morphology EB. This increased cell death rate could also be an indication that some RSCs cannot undergo the differentiation process, dying instead. In any case, while the suggestions for why this occurs are not certain, our results showed that, when in comparison with ESCs, RSCs are significantly less efficient in the process of PrE formation.

Table 3.1 - **Results for embryoid bodies model for Primitive endoderm differentiation, at 96h, represented as percentual values** (based on Table 6.13)**.** Percentual values of: EBs with round morphology, live EBs and Gata6::GFP expressing EBs (EB GFP+) regarding the total number of EBs per condition,; increase of Gata6::GFP expressing EBs from 72h to 96h; and Gata6::GFP expressing EBs with a round morphology relative to the total number of Gata6::GFP expressing EBs. All experimental replicates represented. Retinoic acid (R.A).

Condition	Replicate	EBs round morphology	EBs GFP+	EBs GFP+ round morphology	GFP increase 72h vs 96h	Live EBs
ESC	A	97.44%	86.74%	99.73%	3.02%	90.23%
	B	89.11%	73.16%	95.50%	7.34%	89.37%
	C	88.66%	79.60%	99.37%	0.50%	81.36%
RSC	A	29.15%	17.30%	87.67%	0.47%	66.35%
	B	19.77%	11.16%	81.25%	6.28%	66.98%
	C	15.40%	12.80%	74.07%	1.66%	50.24%
ESC -R.A	A	99.77%	0.00%	0.00%	0.00%	99.07%
	B	99.74%	0.00%	0.00%	0.00%	98.97%
	C	99.77%	0.00%	0.00%	0.00%	100.00%
RSC -R.A	A	97.59%	0.00%	0.00%	0.00%	97.59%
	B	95.18%	0.00%	0.00%	0.00%	96.78%
	C	89.30%	0.00%	0.00%	0.00%	98.37%
ESC -LIF	A	90.47%	84.42%	96.69%	1.86%	81.63%
	B	77.91%	65.29%	93.68%	5.81%	80.83%
	C	68.61%	67.88%	89.61%	0.00%	81.51%
RSC -LIF	A	19.44%	15.46%	78.79%	2.34%	65.81%
	B	19.77%	8.75%	62.86%	1.00%	70.25%
	C	5.58%	4.85%	71.43%	-0.03%	70.47%
RSC (48h in 2i)	A	95.12%	63.26%	98.53%	2.56%	83.49%
	B	88.94%	42.82%	98.90%	6.82%	83.29%
	C	85.58%	63.02%	94.46%	7.21%	87.91%

Table 3.2 - **Levene's test (**for homoscedasticity) **and T-test** (parametric) **or U Mann-Whitney** (non-parametric) **for embryoid bodies model for Primitive endoderm differentiation data presented in Table 3.1 regarding ESC, RSC and RSC (48h in 2i) conditions in all categories and ESC and RSC conditions without retinoic acid in the "EBs round morphology" category.** Parametric and non-paramentric tests performed according to fulfilled assumptions for data normality (Table 6.18) and homoscedasticity assumptions. Levene's test null hypothesis (H0): the groups variances are equal; U Mann-Whitney /T-test null hypothesis (H0): there is no significant difference in the compared conditions for the tested category. Degrees of freedom (Df). Alpha=0.05. Reject H0 if significance (p-value) < 0.05. Levene's test was not calculated for RSC (48h in 2i) due to lack of data normality (Table 6.16).

Category	Conditions compared		Levene's test		T-test			U Mann-Whitney test	
			Statistic	Significance	Statistic	Df	Significance	Statistic	Exact Significance
EBs round Morphology	ESC	RSC	0.43	0.548	14.179	4	0		
		RSC (48h in 2i)						3	0.7
	ESC - R.A	RSC - R.A	8.903	0.041				0	0.1
EBs GFP+	ESC	RSC	0.94	0.387	15.262	4	0		
		RSC (48h in 2i)						0	0.1
EBs GFP+ round morphology	ESC	RSC	1.593	0.275	4.141	4	0.014		
		RSC (48h in 2i)						2	0.4
% GFP increase 72hvs96h	ESC	RSC	0.019	0.896	0.307	4	0.774		
		RSC (48h in 2i)						4	1
% live EBs	ESC	RSC	2.927	0.162	4.186	4	0.014		
		RSC (48h in 2i)						3	0.7

For the condition RSC (48h in 2i), the results revealed an intermediate level in terms of Gata6::GFP expression between ESC and RSC standard conditions, while not significantly different from neither (Table 3.1, 3.2). The difference observed between the RSC (48h in 2i) and the ESC standard condition could indicate that the RSCs did not fully revert to the naïve state and a period longer than 48h in 2i media might be needed. Altogether, these results revealed that the reversion of RSCs seems to recover, to a great extent, the PrE induction ability. This indicates that an epigenetic barrier to the PrE differentiation does not seem to be present in RSCs.

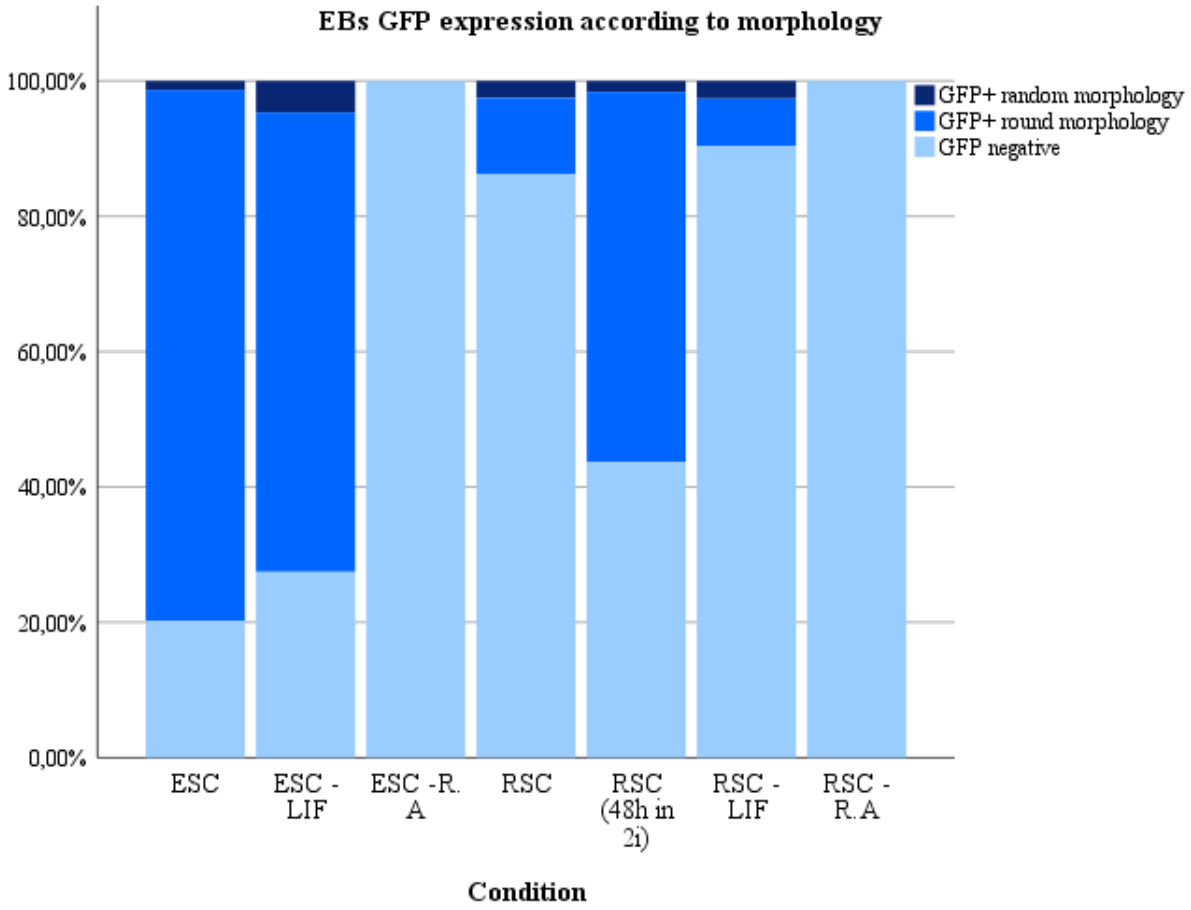

Figure 3.5 – **Percentual embryoid bodies (EBs) Gata6::GFP expression, grouped by morphology, at 96h representation for embryoid bodies model for Primitive endoderm differentiation data**. Values presented in Table 3.1, grouped by both GFP expression (GFP+ random morphology, GFP+ round morphology, GFP Negative) and EB morphology (GFP+ random morphology, GFP+ round morphology) for all ESCs and RSCs conditions: standard, without LIF (-LIF) and without retinoic acid (-R.A). Based on mean values from all replicates.

Secondly, to evaluate the effect of LIF and R.A in the PrE differentiation, differences between the conditions of the same cell type were assessed. We proceeded with the non-parametric Kruskal-Wallis test and a post-hoc Dunn's test, after testing for assumptions (see supplements, Table 6.18). To avoid false negatives, resulting from the conservative nature of the Bonferroni correction for multiple comparisons applied to Dunn's test results, the results that presented significance (p-value<0.05) before the Bonferroni correction were confirmed. A student's t-test or U Mann-Whitney test was performed, according to the required assumptions.

The results revealed significantly lower levels of Gata6::GFP expression in both cell types in the absence of retinoic acid, when comparing to the conditions with the highest Gata6::GFP expression levels: standard ESC and RSC (48h in 2i) (Table 3.1, 3.3, 3.4, 3.5). This supports the previously described role of retinoic acid as the inducing factor for PrE differentiation in the essay (Niakan, K., Schrode, N., Cho, L., *et al*. 2013; Cho, L,. Wamaitha, S., Tsai, I. *et al*. 2012).

A lower proportion of round shaped EBs was observed in the absence of LIF in comparison to other conditions of the same cell type (Table 3.1), significantly in the case of the RSC condition without retinoic acid (Table 3.4). LIF was described to promote a selective effect for ESCs differentiation into

primitive endoderm by inhibiting other cell fates (Shen, M., Leder, P. 1992; Brickman, J., Serup, P. 2017). However, our results support a hypothesis where LIF interferes in the ability of the cells to form and/or maintain the EBs' integrity, that leads to a consequent decrease in Gata6 expression (Table 3.1). While the ability of RSCs to form round EBs is decreased when undergoing PrE differentiation, the removal of LIF accentuates this effect, reflecting its role. This justifies the significant difference observed between the RSC condition without LIF and the RSC condition without retinoic acid, where the proportion of round EBs is higher since no differentiation is occurring.

The results from both PrE differentiation essays presented, revealed that RSCs are able to derive cells that express markers of a primitive endoderm gene profile. However, they express it, in the case of Gata6, in a significantly lower level than ESCs (Niakan, K., Schrode, N., Cho, L., *et al*. 2013; Cho, L,. Wamaitha, S., Tsai, I. *et al*. 2012; Vrij, E., Scholte op Reimer, Y., Frias Aldeguer, J., *et al*. 2019). In summary, our results have shown that when in a differentiation environment, RSCs are significantly less efficient in the process of PrE formation when in comparison to ESCs.

Table 3.3 – **Non-parametric Kruskal-Wallis test and post-hoc Dunn test results for embryoid bodies model for Primitive endoderm differentiation data presented in Table 3.1 referring to all ESCs conditions**. Kruskal-Wallis test H0: there is no significant difference between the grouped ESCs conditions in the tested category. Dunn test H0: in this chosen category, there is no significant difference between the two tested conditions. Alpha = 0.05. Reject H0 if significance (p-value) < 0.05. Degrees of freedom (Df). Retinoic acid (R.A). * significance adjusted with Bonferroni correction for multiple comparisons.

Category	Kruskal-Wallis test			Conditions compared		Post-hoc Dunn test		
	Statistic	Df	Significance			Statistic	Significance	Adj. Significance*
EBs round Morphology	5.956	2	0.051					
EBs GFP+	6.161	2	0.046	ESC	ESC -R.A	5.333	0.015	0.092
					ESC -LIF	1.667	0.448	1
				ESC -	ESC -LIF	3.667	0.095	0.572
EBs GFP+ round morphology	6.713	2	0.035	ESC	ESC -R.A	5.667	0.01	0.06
					ESC -LIF	2.333	0.289	1
				ESC -	ESC -LIF	3.333	0.129	0.777
% GFP increase 72hvs96h	4.582	2	0.101					
% live EBs	5.956	2	0.051					

Table 3.4 - **Non-parametric Kruskal-Wallis test and post-hoc Dunn test results for embryoid bodies model for Primitive endoderm differentiation data presented in Table 3.1 referring to all RSCs conditions**. Kruskal-Wallis test H0: there is no significant difference between the grouped ESCs conditions in the tested category. Dunn test H0: in this chosen category, there is no significant difference between the two tested conditions. Alpha = 0.05. Reject H0 if significance (p-value)< 0.05. Degrees of freedom (Df). Retinoic acid (R.A). * significance adjusted with Bonferroni correction for multiple comparisons.

Category	Kruskal-Wallis test			Conditions compared		Post-hoc Dunn test		
	Statistic	Df	Significance			Statistic	Significance	Adj. Significance*
EBs round Morphology	9.173	3	0.027	RSC	RSC -R.A	-6.5	0.027	0.162
					RSC -LIF	1.333	0.65	1
					RSC (48h in 2i)	-4.167	0.156	0.937
				RSC -R.A	RSC -LIF	-7.833	0.008	0.046
					RSC (48h in 2i)	-2.333	0.427	1
				RSC -LIF	RSC (48h in 2i)	5.5	0.061	0.368
EBs GFP+	9.804	3	0.02	RSC	RSC -R.A	5.333	0.068	0.409
					RSC -LIF	1.667	0.569	1
					RSC (48h in 2i)	-3.667	0.21	1
				RSC -R.A	RSC -LIF	3.667	0.21	1
					RSC (48h in 2i)	9	0.002	0.012
				RSC -LIF	RSC (48h in 2i)	5.333	0.068	0.409
EBs GFP+ round morphology	10.116	3	0.018	RSC	RSC -R.A	5.667	0.053	0.315
					RSC -LIF	2.333	0.425	1
					RSC (48h in 2i)	-3.333	0.254	1
				RSC -R.A	RSC -LIF	3.333	0.254	1
					RSC (48h in 2i)	9	0.002	0.012
				RSC -LIF	RSC (48h in 2i)	5.667	0.053	0.315
% GFP increase 72hvs96h	7.619	3	0.055					
% live EBs	9.667	3	0.022	RSC	RSC -R.A	-8.333	0.005	0.028
					RSC -LIF	-1.667	0.571	1
					RSC (48h in 2i)	-5.333	0.07	0.42
				RSC -R.A	RSC -LIF	-6.667	0.024	0.141
					RSC (48h in 2i)	-3	0.308	1
				RSC -LIF	RSC (48h in 2i)	3.667	0.213	1

Table 3.5 - **Levene's test (**for homoscedasticity) **t-test or U Mann-Whitney for embryoid bodies model for Primitive endoderm differentiation data presented in Table 3.1 regarding ESC, RSC, ESC -R.A, RSC -R.A and RSC -LIF conditions, to confirm statistical adjusted significance** attributed through Dunn test with Bonferroni correction (Table 3.3, 3.4). Parametric and non-parametric tests performed according to fulfilled assumptions for data normality (Table 6.18) and homoscedasticity assumptions. Levene's test null hypothesis (H0): the groups variances are equal; U Mann-Whitney /T-test null hypothesis (H0): there is no significant difference in the compared conditions for the tested category. Degrees of freedom (Df). Alpha=0.05. Reject H0 if significance (p-value) < 0.05. Retinoic acid (R.A).

Category	Conditions compared		Levene's test		T-test			U Mann-Whitney test	
			Statistic	Significance	Statistic	Df	Significance	Statistic	Exact Significance
EBs round Morphology	RSC	RSC - R.A	0.913	0.393	-15.303	4	0		
EBs GFP+	ESC	ESC - R.A	4.444	0.103	20.356	4	0		
EBs GFP+ round	ESC	ESC - R.A	15.168	0.018				0	0.1
% live EBs	RSC - R.A	RSC - LIF	6.77	0.06	18.128	4	0		

3.2. Embryonic diapause *in-vitro* inhibitor induction

The biological process of diapause was replicated *in-vitro* with ESCs. However, it is not known if RSCs are able to enter this state that, *in vivo*, occurs in an embryonic developmental period when rosette stage pluripotency is still not established. To test the response of RSCs when induced into a diapause-like state, we used iMyc and imTOR, shown to induce this dormant state (Scognamiglio, R., Cabezas-Wallscheid, N., Thier, M.C. *et al.* 2016; Bulut-Karslioglu, A., Biechele, S., Jin, H., *et al.* 2016).

iMyc and imTOR impact on cell expansion after 24h treatment

To assess cell expansion, after a 24h culture period for both the conditions with the inhibitors and the controls (cells grown in rosette or 2i medium, without iMyc or imTOR), a cell count was performed. The duration of the treatment with the inhibitors was established at 24h, after an initial trial of a 48h treatment from which no cells were retrieved from the RSCs conditions with the inhibitors, particularly the imTOR (not shown).

The cell number fold increase, which reflects the cell expansion, was calculated as the ratio between the number of cells at 24h and the initial number of cells, in each condition (see supplements, Table 6.19, 6.20). For comparison purposes, the cell number fold increase of the conditions with inhibitors was normalized against the respective controls, RSC for RSC+iMyc/RSC+imTOR and ESC for ESC+iMyc/ESC+imTOR (see supplements, Table 6.21).

No significant differences in the cell number fold increase were found between replicates (Table 6.22).

For the conditions with the inhibitors, in the case of arrest of cell proliferation, the cell number fold increase was expected to be close to half of what is observed in the controls, since cells would not

duplicate. Values lower than that could reflect other effects caused by the inhibitors, such as an increase in cell death.

The results revealed that both iMyc and imTOR suppressed cell expansion in ESCs, and to a significantly larger extent in RSCs (Figure 3.6). Several factors might influence this variable, such as the slightly lower proliferation rate of RSCs (Neagu, A., van Genderen, E., Escudero, I., *et al*. 2020). Nonetheless, an association could be made between the larger suppression observed in RSCs and a more pronounced effect of the inhibitors in regard to cellular arrest and even cell death (Scognamiglio, R., Cabezas-Wallscheid, N., Thier, M.C. *et al.* 2016; Bulut-Karslioglu, A., Biechele, S., Jin, H., *et al*. 2016). Furthermore, the effects of both the inhibitors in the cellular expansion were tested but no consistent significant differences were found between them. The conditions treated with imTOR revealed a lower cell number fold increase, however this difference was not significantly consistent between replicates (see supplements, Table 6.24).

Wnt/β-catenin signaling was recently described as essential for the maintenance of embryonic diapause, by preventing the cell polarization and rosette formation associated with the rosette stage epiblast (Fan, R., Kim, Y., Wu, J., *et al*. 2020; Neagu, A., van Genderen, E., Escudero, I., *et al*. 2020). A hypothesis could be made whether its absence in RSCs might lead to a decreased ability of these cells to undergo or maintain diapause, which would cause an increase in cell death when induced into this process.

We hypothesize that iMyc and imTOR suppress cell expansion through cell growth arrest in ESCs and RSCs (Scognamiglio, R., Cabezas-Wallscheid, N., Thier, M.C. *et al.* 2016; Bulut-Karslioglu, A., Biechele, S., Jin, H., *et al*. 2016). However, we suggest that RSCs might be more susceptible to this induction in comparison to ESCs, with part of the suppression observed caused by a higher cell death rate. An alternative hypothesis could be that in the case of RSCs, the suppression of cell expansion in the conditions with iMyc and imTOR is caused exclusively by cell death, with no cellular growth arrest occurring. This could be tested with a follow-up cell proliferation essay, such as BrdU labelling, to confirm the occurrence, or not, of cellular growth arrest.

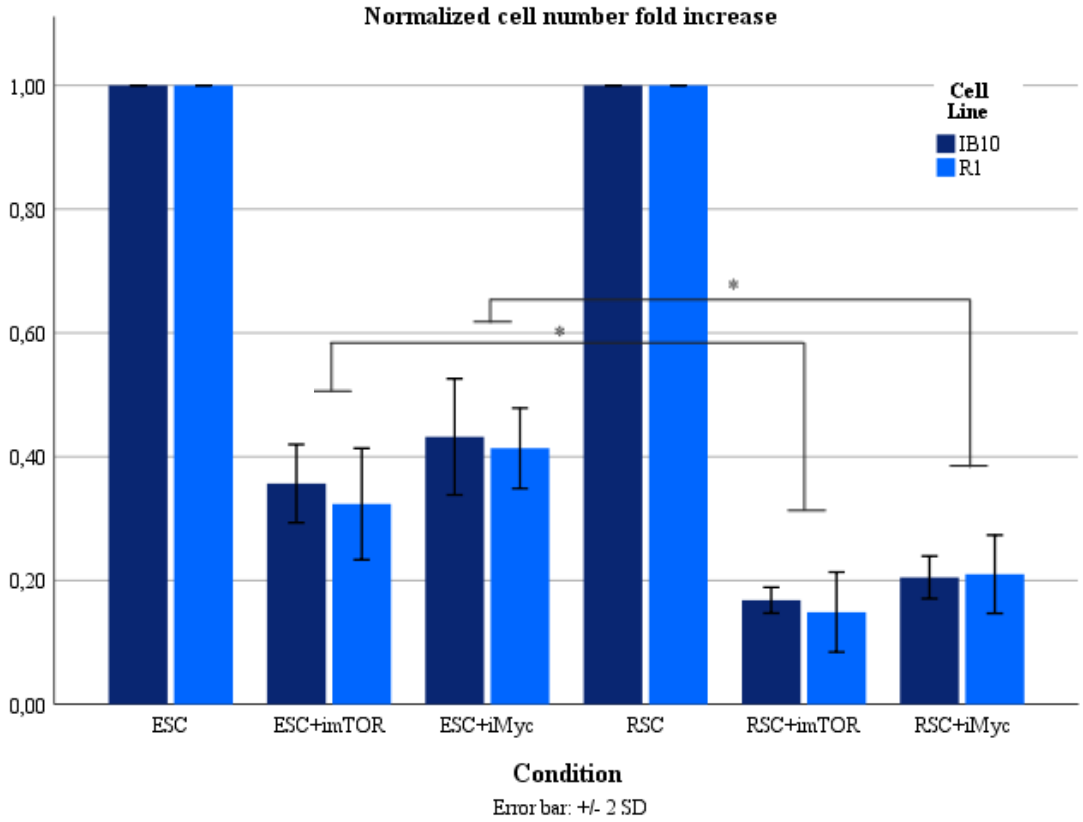

Figure 3.6 – **Normalized cell number fold increase against respective control, for all conditions after 24h treatment with iMyc or imTOR.** (ESC+iMyc and ESC+imTOR normalized against ESC, RSC+iMyc and RSC+imTOR normalized against RSC). The cell number fold increase (Table 6.21) was calculated by dividing the volume corrected cell count with the nº of initial cells plated. All three replicates from R1 and IB10 cell lines are represented. Standard deviation represented by error bar. *statistical analysis shows significant difference, with p-value < 0.05 (Table 6.24).

Ability to form pluripotent colonies after recovery from iMyc and imTOR treatments

The capacity of the cells to exit the dormant state is a fundamental characteristic of the embryonic diapause. As such, we evaluated if after the treatment with the inhibitors, the cells would still maintain their ability to form undifferentiated pluripotent colonies (Fenelon, J., Banerjee, A., Murphy, B. 2014). For this, after the initial 24h treatments with iMyc or imTOR, the cells were trypsinized and passaged at clonal density (200 cells per cm^2), into 2i media. After 72h, the cultures were fixed and stained with alkaline-phosphatase. Untreated ESCs and RSCs were used as controls.

Virtually all the colonies that formed retained their pluripotency and were positive for the ESC marker alkaline phosphatase (see supplements, Table 6.25). While fewer colonies were obtained from RSCs than from ESCs, the inhibitors reduced the colony number to a similar extent for both cell types (Figure 3.7). It is important to refer that plating efficiency may diverge and affect the total number of colonies differently in each condition. However, while not quantified, when fixed, some colonies detached in the conditions treated with inhibitors, particularly in the RSC with imTOR condition.

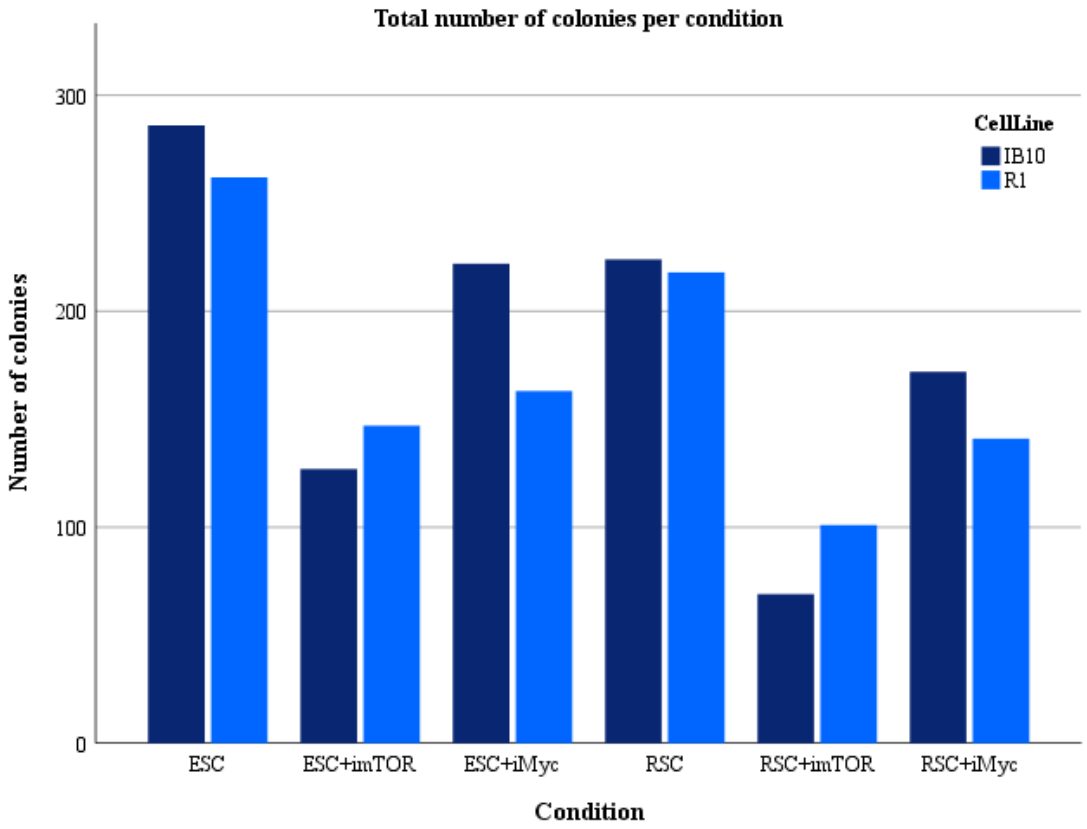

Figure 3.7 - **Embryonic diapause experiment total number of colonies** (Table 6.25) **72h after plating ESCs and RSCs from iMyc, imTOR and control conditions, in 2i media, at clonal density** (400 cells for a single 24-well).

Both in ESC and RSC controls, the total number of colonies was larger than in the respective conditions with the inhibitors. This, associated with the detachment of colonies observed, might reveal some difficulty from the cells to recover and form colonies after the treatments with the inhibitors.

Overall, the results indicate that iMyc and imTOR suppressed cell expansion in both ESCs and RSCs, while to a significantly larger extent in RSCs. Furthermore, both cell types maintained their ability to form undifferentiated pluripotent colonies after recovery from the inhibitor treatment. Hereby, we suggest that the observed difference between cell types might result from a cumulative effect of cell growth arrest and a higher cell death rate in RSCs, due to the absence of Wnt/β-catenin signaling in these cells (Neagu, A., van Genderen, E., Escudero, I., *et al*. 2020; Fan, R., Kim, Y., Wu, J., *et al*. 2020). We hypothesize that, while not null, RSCs ability to undergo a diapause-like state might be significantly reduced in comparison to ESCs.

3.3. Metabolic profile characterization

The metabolic shift that occurs during pluripotency progression alters the metabolic profile of stem cells from a bivalent OxPhos/Glycolytic system in the naïve state (ESCs) to an exclusively highly glycolytic system in the primed state (EpiSCs) (Gatie, M., Kelly, G. 2018; Zhou, W., Choi, M., Margineantu, D. *et al*. 2012).

To evaluate the OxPhos activity of RSCs, they were analyzed, alongside with ESCs (Zhou, W., Choi, M., Margineantu, D. *et al*. 2012). This was achieved by measuring OCR levels of the cells with a Seahorse Extracellular Flux analyzer assay, which refers to mitochondrial respiration.

Initially, the cell number and FCCP concentration were optimized for both ESCs and RSCs. According to the results (see supplements, Figure 6.1), the optimal cell number was of 1E+05 cells and, while the results were not as conclusive, the optimal FCCP concentration was of 2.0µM.

The results between replicates (CGR8 and IB10) did not show consistent values, due to an experimental error in the number of cells plated (Figure 3.8; see supplements, Figure 6.2). Nonetheless, both revealed a clear trend with the RSCs presenting lower values than ESCs for both basal and maximal respiratory capacity, which translates in a lower OCR mean (Figure 3.8). After the inhibition of mitochondrial respiration with antimycin A, ESCs and RSCs showed very similar levels. This confirms that the OCR differences observed were due to OxPhos activity and not to non-mitochondrial respiration processes.

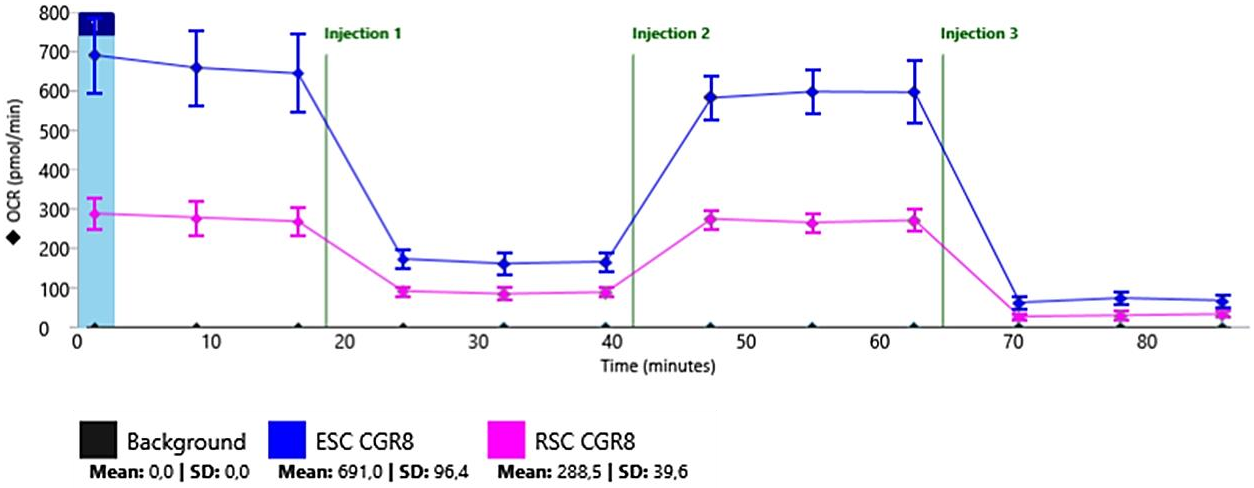

Figure 3.8 - **Seahorse Extracellular Flux analyzer assay OCR measurements for ESC and RSC, CGR8 cell line.** FCCP 2.0µM, and 1E+05 cells. Plotted OCR (oxygen consumption rate) values represent mean of five wells per each density. Injection 1: oligomycin 1µM, Injection 2: FCCP 2.0µM, , Injection 3: antimycin A 1µM. SD (standard deviation). Basal respiratory capacity corresponds to the OCR measurements before injection 1. Maximal respiratory capacity corresponds to the OCR measurements between injection 2 and 3.

The spare respiratory capacity is calculated as the difference between maximal and basal respiratory levels. It reflects the amount of ATP the cell can produce through OxPhos in case of an extra energy demand, for example in a situation of stress (Desler, C., Hansen, T., Frederiksen, J., *et al*. 2012). The presence of spare respiratory capacity was inconclusive in ESCs due to different results between the cell lines tests (see supplements, Figure 6.2; Figure 3.8). In the case of RSCs, the non-existence of spare respiratory capacity was confirmed in both replicates. This indicates that if extra ATP is required, RSCs will not be able to produce it through the OxPhos pathway, which suggests that the cells might recur to another pathway or show a quiescent metabolic profile.

One other factor suggested to impact the metabolic shift during the transition from the naïve to primed state is the downregulation of cytochrome c oxidase family genes, essential for aerobic respiration (Fontanesi, F., Soto, I., Barrientos, A., *et al*. 2008; Zhou, W., Choi, M., Margineantu, D. *et al*. 2012). To test if such downregulation occurred in RSCs, a gene set enrichment analysis (GSEA) was performed based on published RNA-Seq data (Neagu, A., van Genderen, E., Escudero, I., *et al*. 2020) with a gene set composed by OxPhos pathway related genes (see List 6.1). The GSEA revealed that the gene set is negatively enriched (p-value 0.021) in RSCs in comparison to ESCs (FDR: 0.021), indicating that oxidative phosphorylation related genes are downregulated in RSCs.

Altogether, lower OCR levels and a consequent lower OxPhos activity was observed in RSCs, in comparison to ESCs. This is consistent with the more developmentally advanced rosette stage, since the metabolic shift is described as an early feature of ESCs progression from naïve pluripotency (Zhou, W., Choi, M., Margineantu, D. *et al*. 2012). The transition from a rich oxygen environment to one that is not, which occurs in primed cells, was indicated as a possible reason for this change in the metabolism. The rosette stage refers to the peri-implantation epiblast, a stage that occurs in the low-oxygen uterus environment, which could explain the decrease of mitochondrial respiration observed in RSCs (Zhou, W., Choi, M., Margineantu, D. *et al*. 2012; Lee, S., S, H., Lee, J., *et al*. 2019). For a complete characterization, an analysis of the glycolic activity is required. Nonetheless, the identified lower levels of mitochondrial respiration in RSCs might reflect a more quiescent metabolic profile, which could lead to cellular characteristics such as the decreased proliferation rate in comparison to naïve stage cells (Neagu, A., van Genderen, E., Escudero, I., *et al*. 2020).

4. Conclusion

The goal of this study was to further characterize the biological properties of RSCs. For that, their performance was assessed when subjected to assays regarding two early-blastocyst biological processes: PrE differentiation and embryonic diapause. This study revealed a loss of developmental potential from RSCs in the aforementioned processes, in comparison to ESCs.

The initial approach focused on the ability to derive primitive endoderm, a cell lineage that *in vivo* starts to be determined with the exclusive expression of Gata6 in the ICM cells (Artus, J., Piliszek, A., *et al*. 2011). Our data revealed that ESCs and RSCs showed significant differences in the response to the PrE differentiation processes. ESCs, as it had been previously described, were able to derive cells that expressed PrE characteristic markers. While it was not an all-or-nothing result, RSCs were also able to form primitive endoderm-like-gata6 expressing cells, however in a significantly less efficient manner (Plusa, B., Piliszek, A., Frankenberg, S., *et al*. 2008).

We hypothesize that the developmental timepoint in which the cell commitment to a PrE fate occurs, could be an underlying cause for the limited potential observed in RSCs, since these cells correlate to the more advanced peri-implantation epiblast (Artus, J., Piliszek, A., *et al*. 2011; Neagu, A., van Genderen, E., Escudero, I., *et al*. 2020). Further studies are required to confirm this limitation, as well as understanding the factors that lead to it. One hypothesis includes the existence of sub-populations of RSCs, due to slightly different developmental timepoints, with cells presenting a more permissive or advanced state. Thereby their timing or ability for PrE differentiation could be affected, with some being able to do it and others not. The first step to address this question would be to assess the presence of sub-populations of RSCs, for example with a fluorescent activated cell sorting analysis. If confirmed, a genetic screening approach could follow, to try to characterize and distinguish the sub-populations detected.

The embryonic diapause assay data also revealed a significantly different response between the rosette and naïve stage cells. Both cell types retained their pluripotent potential after the diapause-inducing treatments. However, RSCs revealed a more accentuated suppression of cell expansion during these treatments, in comparison to ESCs. We hypothesize that RSCs have a reduced ability to enter a diapause-like state. We suggest that this could result from the absence of Wnt/β-catenin signaling in RSCs, described as an essential factor in the diapaused embryo maintenance (Fenelon, J., Banerjee, A., Murphy, B. 2014). This would result in an increase in cell death when the cells are induced into this state (Neagu, A., van Genderen, E., Escudero, I., *et al*. 2020; Fan, R., Kim, Y., Wu, J., *et al*. 2020).

Wnt/β-catenin signaling activation reverts RSCs to a naïve state and is simultaneously essential for diapause maintenance. For a follow-up study, it would be interesting to explore what occurs in the RSCs that survive the diapause-inducing process and retain their pluripotent potential (Fan, R., Kim, Y., Wu, J., *et al*. 2020; Neagu, A., van Genderen, E., Escudero, I., *et al*. 2020). Could it be that the forced diapause-induction with inhibitors leads to an activation of the Wnt/β-catenin pathway in some of these cells? If so, are these cells reverting to a naïve state? An option to approach these questions would be through an assessment of this pathway's activity levels in the RSCs that survive the diapause-inducing treatments, by analyzing Wnt and β-catenin expression.

Naïve and primed stem cells are associated with a specific metabolic profile. While ESCs present a bivalent system with both OxPhos and glycolytic activity, EpiSCs have an exclusively highly glycolytic system (Scognamiglio, R., Cabezas-Wallscheid, N., Thier, M.C. *et al.* 2016). Due to the

importance associated to the metabolic shift during pluripotency progression, we aimed to establish the activity of the OxPhos pathway in RSCs. These cells revealed a lower oxygen consumption rate, in comparison to ESCs.

The lower OxPhos activity together with the observed downregulation in oxidative phosphorylation related genes in RSCs, a process also seen in primed cells, indicates a different metabolic profile between RSCs and ESCs. This aligns with the described metabolic reset that occurs when naïve cells transition to a primed pluripotency state, which supports the characterization of RSCs as representatives of a more advanced pluripotent stage (Zhou, W., Choi, M., Margineantu, D. *et al*. 2012). For a more complete characterization of RSCs ATP-production pathways, it would be important to analyze their glycolytic activity, by performing a seahorse glycolysis stress test. This would allow for a comparison with the primed cells and an overall distinction of the metabolic profiles of the different pluripotent stages. A follow-up experiment could focus on the assessment of the mitochondria morphology of RSCs. This distinct characteristic between naïve and primed cells is directly associated with their metabolic profile (Zhou, W., Choi, M., Margineantu, D. *et al*. 2012).

Altogether, this work broadens the characterization of RSCs, by establishing differences in regard to their developmental potential and metabolic profile from the extensively characterized ESCs.

The progress of fundamental research is key in the path for broader applications, with stem cell biology not being an exception. The therapeutic and medical applications of stem cells are already a reality, with contributions in several areas. Examples include the use of organoids for drugs and disease screening, tissue engineering and reparation, and more specific applications such as insulin therapy (Mahla, R. 2016). However, there are still missing links. The fact that induced pluripotent stem cells tend to differentiate into the lineage from which they were derived is a good example that there is still a lot to be learned about pluripotency and the way we reprogram it (Hu, S., Zhao, M., Jahanbani, F., *et al*. 2016). Pluripotency progression works as a continuum that is critical for the success of the embryo development and, consequently, will impact all other processes depending on it. Filling the missing steps that form this continuum is, for that reason, essential for a better and improved application of stem cells' full pluripotent potential.

5. References

Agilent Technologies. Agilent Seahorse XF Cell Mito Stress Test Kit User Guide Kit 103015-100.

Artus, J., Piliszek, A., Hadjantonakis, A. K. The primitive endoderm lineage of the mouse blastocyst: Sequential transcription factor activation and regulation of differentiation by Sox17. *Developmental Biology.* **350**, 393–404 (2011).

Bernstein, B., Mikkelsen, T., Xie, X., Kamal, M., Huebert, D., Cuff, J., Fry, B., Meissner, A., Wernig, M., Plath, K., Jaenisch, R., Wagschal, A., Feil, R., Schreiber, S., Lander, E. Bivalent Chromatin Structure Marks Key Developmental Genes in Embryonic Stem Cells. *Cell* . **125**, 315–326 (2006).

Bio-Rad Laboratories. iTaq Universal SYBR Green Supermix.

Brickman, J., Serup, P. Properties of embryoid bodies. *Wiley Interdisciplinary Reviews Developmental Biology.* **6** (2017).

Brons, I., Smithers, L., Trotter, M., Rugg-Gunn, P., Sun, B., Chuva De Sousa Lopes, S., Howlett, S., Clarkson, A., Ahrlund-Richter, L., Pedersen, R., Vallier, L. Derivation of pluripotent epiblast stem cells from mammalian embryos. *Nature* **448**, 191–195 (2007).

Bulut-Karslioglu, A., Biechele, S., Jin, H., MacRae, T., Hejna, M., Gertsenstein, M., Song, J., Ramalho-Santos, M. Inhibition of mTOR induces a paused pluripotent state. *Nature* **540**, 119–123 (2016).

Cai, K., Capo-Chichi, C., Rula, M., Yang, D., Xu, X. Dynamic GATA6 expression in primitive endoderm formation and maturation in early mouse embryogenesis. *Developmental Dynamics.* **237**, 2820–2829 (2008).

Cho, L., Wamaitha, S., Tsai, I., Artus, J., Sherwood, R., Pedersen, R., Hadjantonakis, A., Niakan, K. Conversion from mouse embryonic to extra-embryonic endoderm stem cells reveals distinct differentiation capacities of pluripotent stem cell states. *Development (Cambridge).* **139**, 2866–2877 (2012).

Desler, C., Hansen, T., Frederiksen, J., Marcker, M., Singh, K., Juel Rasmussen, L. Is there a link between mitochondrial reserve respiratory capacity and aging? *Journal of Aging Research* (2012).

Deuve, J., Avner, P. The coupling of X-chromosome inactivation to pluripotency. *Annual Review Cell Developmental Biology.* **27**, 611–629 (2011).

Fan, R., Kim, Y., Wu, J., Chen, R., Zeuschner, D., Mildner, K., Adachi, K., Wu, G., Galatidou, S., Li, J., Schöler, H., Leidel, S., Bedzhov, I. Wnt/Beta-catenin/Esrrb signalling controls the tissue-scale reorganization and maintenance of the pluripotent lineage during murine embryonic diapause. *Nature Communications.* **11**, 1–17 (2020).

Fenelon, J., Banerjee, A., Murphy, B. Embryonic diapause: development on hold. *International Journal of Developmental Biology*. **58**, 163–174 (2014).

Fontanesi, F., Soto, I., Barrientos, A. Cytochrome c oxidase biogenesis: New levels of regulation. *IUBMB Life.* **60**, 557–568 (2008).

Freyer, L., Schröter, C., Saiz, N., Schrode, N., Nowotschin, S., Martinez-Arias, A., Hadjantonakis, A. A loss-of-function and H2B-Venus transcriptional reporter allele for Gata6 in mice Early development. *BMC Developmental Biology.* **15**, 38 (2015).

Gatie, M. I., Kelly, G. M. Metabolic profile and differentiation potential of extraembryonic endoderm-like cells. *Cell Death Discovery.* **4**, (2018).

Hassani, S., Totonchi, M., Gourabi, H., Schöler, H., Baharvand, H. Signaling roadmap modulating naive and primed pluripotency. *Stem Cells and Development.* **23**, 193–208 (2014).

Hayashi, K., Ohta, H., Kurimoto, K., Aramaki, S., Saitou, M. Reconstitution of the Mouse Germ Cell Specification Pathway in Culture by Pluripotent Stem Cells. *Cell.* **146**, 519–532 (2011).

Hermitte, S., Chazaud, C. Primitive endoderm differentiation: From specification to epithelium formation. *Philosophical Transactions of the Royal Society B: Biological Sciences*. **369** (2014).

Hu, S., Zhao, M.-T., Jahanbani, F., Shao, N.-Y., Lee, W., Chen, H., Snyder, M., Wu, J. Effects of cellular origin on differentiation of human induced pluripotent stem cell–derived endothelial cells. *JCI Insight* **1** (2016).

Hurlin, P. J. N-myc functions in transcription and development. *Birth Defects Research Part C: Embryo Today: Reviews.* **75**, 340–352 (2005).

Hussein, A., Wang, Y., Mathieu, J., Margaretha, L., Song, C., Jones, D., Cavanaugh, C., Miklas, J., Mahen, E., Showalter, M., Ruzzo, W., Fiehn, O., Ware, C., Blau, C., Ruohola-Baker, H. Metabolic Control over mTOR-Dependent Diapause-like State. *Developmental Cell*. **52**, 236-250 (2020).

Kalkan, T., Olova, N., Roode, M., Mulas, C., Lee, H., Nett, I., Marks, H., Walker, R., Stunnenberg, H., Lilley, K., Nichols, J., Reik, W., Bertone, P., Smith, A. Tracking the embryonic stem cell transition from ground state pluripotency. *Development (Cambridge).* **144,** 1221-1234 (2017).

Kang, M., Piliszek, A., Artus, J., Hadjantonakis, A. FGF4 is required for lineage restriction and salt-and-pepper distribution of primitive endoderm factors but not their initial expression in the mouse. *Development (Cambridge).* **140**, 267–279 (2013).

Kojima, Y., Tam, O., Tam, P. Timing of developmental events in the early mouse embryo. *Seminars in Cell and Developmental Biology*. **34**, 65–75 (2014).

Lee, S., Seo, H., Lee, J., Jun, J., Choi, K. Effects of dynamic oxygen concentrations on the development of mouse pre- and peri-implantation embryos using a double-channel gas supply incubator system. *Clinical and Experimental Reproductive Medicine.* **46**, 189–196 (2019).

Liu, W., Cheng, R., Niu, Z., Chen, A., Ma, M., Li, T., Chiu, P., Pang, R., Lee, Y., Ou, J., Yao, Y., Yeung, W. Let-7 derived from endometrial extracellular vesicles is an important inducer of embryonic diapause in mice. *Science Advances*. **6** (2020).

Mahla, R. Stem cells applications in regenerative medicine and disease therapeutics. *International Journal of Cell Biology*. (2016).

Martello, G., Smith, A. The Nature of Embryonic Stem Cells. *Annual Review of Cell and Developmental Biology*. **30**, 647–675 (2014).

Neagu, A., van Genderen, E., Escudero, I., Verwegen, L., Kurek, D., Lehmann, J., Stel, J., Dirks, R., van Mierlo, G., Maas, A., Eleveld, C., Ge, Y., den Dekker, A., Brouwer, R., van IJcken, W., Modic, M., Drukker, M., Jansen, J., Rivron, N., ten Berge, D. In vitro capture and characterization of embryonic rosette-stage pluripotency between naive and primed states. *Nature. Cell Biology.* **22**, 534–545 (2020).

Niakan, K., Schrode, N., Cho, L., Hadjantonakis, A. K. Derivation of extraembryonic endoderm stem (XEN) cells from mouse embryos and embryonic stem cells. *Nature Protocols*. **8**, 1028–1041 (2013).

Osorno, R., Tsakiridis, A., Wong, F., Cambray, N., Economou, C., Wilkie, R., Blin, G., Scotting, P., Chambers, I., Wilson, V. The developmental dismantling of pluripotency is reversed by ectopic Oct4 expression. *Developmental (Cambridge)*. **139**, 2288–2298 (2012).

Pauklin, S., Vallier, L. Activin/nodal signalling in stem cells. *Development (Cambridge)*. **142**, 607–619 (2015).

Plusa, B., Piliszek, A., Frankenberg, S., Artus, J. & Hadjantonakis, A. K. Distinct sequential cell behaviours direct primitive endoderm formation in the mouse blastocyst. *Development* **135**, 3081–3091 (2008).

Ptak, G., Tacconi, E., Czernik, M., Toschi, P., Modlinski, J., Loi, P. Embryonic Diapause Is Conserved across Mammals. *PLoS One* **7**, e33027 (2012).

QIAGEN. RNeasy Mini Handbook. (2019).

Renfree, M., Fenelon, J. C. The enigma of embryonic diapause. *Development (Cambridge)*. **144**, 3199–3210 (2017).

Rizzino, A. The Sox2-Oct4 connection: Critical players in a much larger interdependent network integrated at multiple levels. *Stem Cells.* **31**, 1033–1039 (2013).

Scognamiglio, R., Cabezas-Wallscheid, N., Thier, M., Altamura, S., Reyes, A., Prendergast, Á., Baumgärtner, D., Carnevalli, L., Atzberger, A., Haas, S., Von Paleske, L., Boroviak, T., Wörsdörfer, P., Essers, M., Kloz, U., Eisenman, R., Edenhofer, F., Bertone, P., Huber, W., Trumpp, A. Myc Depletion Induces a Pluripotent Dormant State Mimicking Diapause. *Cell.* **164**, 668–680 (2016).

Shen, M., Leder, P. Leukemia inhibitory factor is expressed by the preimplantation uterus and selectively blocks primitive ectoderm formation in vitro. *Proceedings of the National Academy of Sciences of the United States of America.* **89**, 8240–8244 (1992).

Shyh-Chang, N., Ng, H. The metabolic programming of stem cells. *Genes and Development*. **31,** 336–346 (2017).

Smith, A. Formative pluripotency: the executive phase in a developmental continuum. *Development*. **144**, 365–373 (2017).

Soprano, D., Teets, B., Soprano, K. Role of Retinoic Acid in the Differentiation of Embryonal Carcinoma and Embryonic Stem Cells. *Vitamins and Hormones*. **75** (2007).

Štefková, K., Procházková, J., Pacherník, J. Alkaline Phosphatase in Stem cells. *Stem Cells International*. (2015).

Subramanian, A., Tamayo, P., Mootha, V., Mukherjee, S., Ebert, B., Gillette, M., Paulovich, A., Pomeroy, S., Golub, T., Lander, E., Mesirov, J. Gene set enrichment analysis: A knowledge-based approach for interpreting genome-wide expression profiles. *Proceedings of the National Academy of Sciences of the United States of America*. **102**, 15545–15550 (2005).

Takahashi, S., Kobayashi, S., Hiratani, I. Epigenetic differences between naïve and primed pluripotent stem cells. *Cellular and Molecular Life Sciences*. **75**, 1191–1203 (2018).

Tee, W. W. & Reinberg, D. Chromatin features and the epigenetic regulation of pluripotency states in ESCs. *Development (Cambridge)*. **141**, 2376–2390 (2014).

Teslaa, T., Teitell, M. Pluripotent stem cell energy metabolism: an update. The *EMBO Journal*. **34**, 138–153 (2015).

Tosolini, M., Jouneau, A. From naive to primed pluripotency: In vitro conversion of mouse embryonic stem cells in epiblast stem cells. in *Methods in Molecular Biology*. **1341**, 209–216 (2015).

Van Der Pluijm, I., Burger, J., Van Heijningen, P., IJpma, A., Van Vliet, N., Milanese, C., Schoonderwoerd, K., Sluiter, W., Ringuette, L., Dekkers, D., Que, I., Kaijzel, E., te Riet, L., MacFarlane, E., Das, D., Van Der Linden, R., Vermeij, M., Demmers, J., Mastroberardino, P., Essers, J. Decreased mitochondrial respiration in aneurysmal aortas of Fibulin-4 mutant mice is linked to PGC1A regulation. *Cardiovascular Research*. **114**, 1776–1793 (2018).

Vrij, E., Scholte op Reimer, Y., Frias Aldeguer, J., Misteli Guerreiro, I., Kind, J., Koo, B.-K., van Blitterswijk, C., Rivron, N. Chemically-defined induction of a primitive endoderm and epiblast-like niche supports post-implantation progression from blastoids. B*ioRxiv* 510396 (2019).

Weinberger, L., Ayyash, M., Novershtern, N., Hanna, J. Dynamic stem cell states: Naive to primed pluripotency in rodents and humans. *Nature Reviews Molecular Cell Biology*. **17**, 155–169 (2016).

Wu, J., Izpisua Belmonte, J. Dynamic Pluripotent Stem Cell States and Their Applications. *Cell Stem Cell*. **17**, 509–525 (2015).

Yang, S. H., Kalkan, T., Morissroe, C., Marks, H., Stunnenberg, H., Smith, A., Sharrocks, A. Otx2 and Oct4 Drive Early Enhancer Activation during Embryonic Stem Cell Transition from Naive Pluripotency. *Cell Reports*. **7**, 1968–1981 (2014).

Yi, F., Pereira, L., Merrill, B. Tcf3 Functions as a Steady-State Limiter of Transcriptional Programs of Mouse Embryonic Stem Cell Self-Renewal. *Stem Cells* **26**, 1951–1960 (2008).

Ying, Q., Wray, J., Nichols, J., Batlle-Morera, L., Doble, B., Woodgett, J., Cohen, P., Smith, A. The ground state of embryonic stem cell self-renewal. *Nature* **453**, 519–523 (2008).

Zhou, W., Choi, M., Margineantu, D., Margaretha, L., Hesson, J., Cavanaugh, C., Blau, C., Horwitz, M., Hockenbery, D., Ware, C., Ruohola-Baker, H. HIF1α induced switch from bivalent to exclusively glycolytic metabolism during ESC-to-EpiSC/hESC transition. The *EMBO Journal*. **31**, 2103–2116 (2012).

6. Supplements

Protocol A

RNeasy Mini Kit (QIAGEN) instructions for "Protocol: Purification of total RNA from Animal Cells using Spin Technology" and "Dnase Digestion with the RNAse-Free Dnase Set"

1. To direct lysis of the cells, add the appropriate amount of RLT buffer (for less than $5*10^6$ cells use 350µl, for a cell number between $5*10^6$ and $1*10^7$ use 600µl) and collect the lysate into a sterilized tube.

2. To homogenize the sample, load up to 700 µl of lysate onto a QIA shredder spin column placed in a 2 ml collection tube, and spin for 2 min at maximum speed in a microcentrifuge. The lysate is homogenized as it passes through the spin column. Keep the collection tube.

3. Add 1 volume of 70% ethanol to the homogenized sample and mix well by pipetting. Do not centrifuge.

4. Transfer up to 700 µl of the sample, including any precipitate that may have formed, to a Rneasy spin column placed in a 2 ml collection tube. Close the lid gently, and centrifuge for 15 s at ≥8000 x g (≥10,000 rpm). Discard the flow-through. Reuse the collection tube in next step.

   The following 4 steps regard Dnase digestion:

   a. Add 350µl Buffer RW1 to the Rneasy spin column. Close the lid gently, and centrifuge for 15 s at ≥8000 x g (≥10,000 rpm) to wash the spin column membrane. Discard the flow-through. Reuse the collection tube in next step.

   b. Add 10 µl Dnase I stock solution to 70µl Buffer RDD. Mix by gently inverting the tube. Centrifuge briefly to collect residual liquid from the sides of the tube.

Note: Dnase I is especially sensitive to physical denaturation. Mixing should only be carried out by gently inverting the tube. Do not vortex.

   c. Add the Dnase I incubation mix (80µl) directly to the Rneasy spin column membrane, and place on the benchtop (20–30°C) for 15 min.

   d. Add 350µl Buffer RW1 to the Rneasy spin column. Close the lid gently, and centrifuge for 15 s at ≥8000 x g (≥10,000 rpm). Discard the flow-through.

5. Add 700µl Buffer RW1 to the Rneasy spin column. Close the lid gently, and centrifuge for 15 s at ≥8000 x g (≥10,000 rpm) to wash the spin column membrane. Discard the flow-through. Reuse the collection tube in the next step.

6. Add 500µl Buffer RPE to the Rneasy spin column. Close the lid gently, and centrifuge for 15 s at ≥8000 x g (≥10,000 rpm) to wash the spin column membrane. Discard the flow-through. Reuse the collection tube in the next step.

7. Add 500µl Buffer RPE to the Rneasy spin column. Close the lid gently, and centrifuge for 2 min at ≥8000 x g (≥10,000 rpm) to wash the spin column membrane.

8. Place the Rneasy spin column in a new 1.5 ml collection tube. Add 30µl RNAse-free water directly to the spin column membrane. Close the lid gently, and centrifuge for 1 min at ≥8000 x g (≥10,000 rpm) to elute the RNA.

9. Close the collection tube. RNA sample is ready to be used or frozen at -20ºC.

Note: All the materials used in this protocol (buffers, Dnase solution, collection tubes, spin columns, etc.) were supplied in Rneasy Mini Kit.

Protocol B

User Guide RevertAid First Strand cDNA Synthesis Kit (Thermofisher)

1. Add the following reagents into a sterile, nuclease- free tube on ice in the indicated order:

   Template RNA: 1µg
   Random Hexamer primer: 1 µL
   Water, nuclease-free up to total volume of 12 µL

2. Add the following components in the indicated order:

   5X Reaction Buffer: 4 µL
   RiboLock Rnase Inhibitor (20 U/µL): 1 µL
   10 mM dNTP Mix: 2 µL
   RevertAid M-MuLV RT (200 U/µL): 1 µL
   Total volume: 20 µL

3. Mix gently and centrifuge briefly.

4. Incubate for 5 min at 25°C followed by 60 min at 42°C.

5. Terminate the reaction by heating at 70°C for 5 min.

6. Dilute cDNA 1:20 in miliwater before using or freezing.

Note: 1) All the materials used in this protocol were supplied in the RevertAid First Strand cDNA Synthesis Kit. **2)** In the case there are samples from which it is not possible to get 1µg of template RNA, use 500 ng and in step 6 dilute the cDNA 1:10 instead to achieve same final cDNA concentration.

Protocol C

iTaq Universal SYBR Green Supermix user guide (Bio-Rad)

Reaction setup:

cDNA: 500 ng
iTaq Universal SYBR Green Supermix: 10 µL
Primer:s 500nM (250 nM of each primer, reverse and forward)
Water, nuclease-free up to total volume of 20 µL

1. Prepare enough mix for all qPCR reactions by adding all required components according to the reaction setup, except the DNA template.

2. Mix the reaction thoroughly and dispense equal aliquots into the wells of a qPCR plate.

3. Add cDNA samples to the wells containing the reaction mix (cDNA and controls -RT).

4. Seal wells with optically transparent film and vortex for 10 seconds to ensure mixing of all components. Spin qPCR plate for 20seconds at maximum speed to remove any air bubbles and collect the reaction mixture in the bottom of the well.

5. Program the thermal cycling protocol (see materials and methodology, 2D Primitive endoderm differentiation assay, qPCR running protocol cycle setup), load the plate and start the run.

Protocol D

Agilent Seahorse XF Cell Mito Stress Test Kit User Guide (Kit 103015-100, Agilent Technologies)

1. Hydrate the sensor cartridge (Extracellular Flux Assay kit) in 1mL XF calibration medium.

6. Seal plate with parafilm and incubate overnight at 37ºC in a non-CO^2 incubator.

Day of the Seahorse assay

2. Prepare assay medium and mito test compounds (oligomycin, FCCP and antimycin A at final concentration in well of 1µM, 2 µM and 1 µM, respectively).

Standard assay medium: XF base medium 48.5 mL
1 mM Pyruvate 0.5 mL (100mM)
2 mM Glutamin 0.5 mL (200mM)
10 mM Glucose 0.5 mL (1M)

3. Wash cells with assay medium:

- Take out 150 µL medium in every well using a multichannel pipet (100 µL medium left).

- Wash with 1mL assay medium (1.1mL total volume).

- Take out 1mL medium (100 µL left).

- Add 475 µL assay medium (575 µL total volume).

4. Incubate at 37C in a non-CO^2 incubator for 60 minutes.
5. Load sensor cartridge ports with the appropriate compounds for the mito test.
6. Pipet the compounds to the side of the ports
   Port A (bottom right): 64 µL Oligomycin (10µM solution)
   Port B (bottom left): 71 µL FCCP (10µM solution)
   Port C (top right): 79 µL Antimycin A (10µM solution)
   Port D (top left): Empty

   The ports of the background wells are loaded with similar amounts of 1% DMSO in assay medium.

7. Incubate loaded sensor cartridge at 37ºC/non-CO^2 for ~10 minutes.
8. Start the Mito test protocol on the Seahorse XF24 machine with the loaded sensor calibration plate ~30 minutes after starting the incubation of the cell plate.

<u>Seahorse XF24 mito stress test cycles</u>

1. Calibrate (after calibration the calibration plate is switched for the cell plate).
2. Equilibrate
3. Loop start (3x)
   Mix 2 min
   Wait 2 min
   Measure 3 min
   Loop end

6. Inject port A
   Loop start (3x)
   Mix 2 min
   Wait 2 min
   Measure 3 min
   Loop end

6. Inject port B
   Loop start (3x)
   Mix 2 min
   Wait 2 min
   Measure 3 min
   Loop end

6. Inject port C
   Loop start (3x)
   Mix 2 min
   Wait 2 min
   Measure 3 min
   Loop end

Note: 1) All reagents required are provided in the Agilent Seahorse XF Cell Mito Stress Test Kit.

2) Compound role: a) Oligomycin blocks ATP synthase, b) FCCP transports protons across the mitochondrial inner membrane, interfering with the proton gradient and thereby uncoupling proton flow from ATP synthesis and c) Antimycin A blocks complex III and thereby disrupts the entire electron transport chain.

Table 6.1 - **N2B27+LIF cell culture media components**

N2B27 medium compounds	Volume
DMEM/F12 + Glutamax	242 mL
Neural basal medium	242 mL
Pen/Strep	5 mL
Glutamax	2.5 mL
B27, serum free	5 mL
N2-supplement B	2.5 mL
Bovine Serum albumin fractionV	160 µL
2-Mercapto-ethanol 50mM	0.5 mL
LIF	50 µL
Total volume	**500 mL**

Table 6.2 - **Number of initial cells seeded at Day0 for the 2D Primitive endoderm differentiation assay according to desired cell density and surface area of culture.**

PrE differentiation day	Cell type	Initial cell seeding density (cells per cm^2)		
		1.00E+04	2.00E+04	3.00E+04
Day 7	ESCs	5.67E+05 [a]	1.9E+05 (x2)[b]	2.85E+05 (x2)[b]
	RSCs	5.67*10^5 [a]	1.13E+06 [a]	1.7E+06 [a]
Day10	ESCs	9.5E+04 (x2)[b]	1.9E+05 (x2)[b]	2.85E+05 (x2)[b]
	RSCs	5.67E+05 [a]	1.13E+06 [a]	2.85E+05 (x2)[b]
Day13	ESCs	9.5E+04 (x2)[b]	1.9E+05 (x2)[b]	2.85E+05 (x2)[b]
	RSCs	5.67E+05 [a]	1.13E+06 [a]	2.85E+05 (x2)[b]
[a] One 10cm dish (55cm^2 area), [b] Two 6 wells (9.5cm^2 each)				

Table 6.3 - **Primer pairs designed in BLAST for PrE markers - Sox17, Gata4, Pdgfrα, naïve pluripotency marker Nanog and housekeeping gene Gapdh used in qPCR analysis of samples from the 2D Primitive endoderm differentiation assay**.

Gene		Primer sequences
Sox17	Foward	5'-GGA GGG TCA CCA CTG CTT TAT-3'
	Reverse	5'-CCA AGA CTT GCC TTG GGG AAA AC-3'
Gata4	Foward	5'-GGA GAT CGC GCC GGT TTT C-3'
	Reverse	5'-ACC TCT AGG CTC TGG TTT GC-3'
Pdgfrα	Foward	5'-CGG AAG GGT GGA ATT TAG GAG G-3'
	Reverse	5'-GGC GTT AAC CAC TTC CAG CA-3'
Nanog	Foward	5'-GCT GAT TTG GTT GGT GTC TTG C-3'
	Reverse	5'- GGT CTT CAG AGG AAG GGC GA-3'
Gapdh	Foward	5'-TAT GAT GAC ATC AAG AAG GTC G-3'
	Reverse	5'-CAT TGT CAT ACC AGG AAA TGA A-3'

Table 6.4 - **Cell number fold increase regarding number of live cells at day 7 in ESCs and RSCs cultures undergoing the 2D Primitive endoderm differentiation assay and initial number of cells seeded**. Three replicates (A, B, C), including cultures with all three initial seeding densities (cells per cm^2): 1E+04, 2E+04 and 3E+04.

Cell type	Replicate	Cell density (cells per cm^2)	Plated surface (cm^2)	Initial cell number	Final cell number	Cell number fold increase
ESCs	A	1.00E+04	55	5.67E+05	1.30E+07	22.89241623
		2.00E+04	9.5	1.90E+05	3.60E+06	18.94736842
		3.00E+04	9.5	2.85E+05	6.92E+06	24.28070175
ESCs	B	1.00E+04	9.5	9.50E+04	1.96E+06	20.63157895
		2.00E+04	9.5	1.90E+05	3.78E+06	19.91578947
		3.00E+04	9.5	2.85E+05	6.36E+06	22.31578947
ESCs	C	1.00E+04	9.5	9.50E+04	1.98E+06	20.8
		2.00E+04	9.5	1.90E+05	3.40E+06	17.89473684
		3.00E+04	9.5	2.85E+05	6.28E+06	22.03508772
RSCs	A	1.00E+04	55	5.67E+05	9.92E+06	17.49559083
		2.00E+04	55	1.11E+06	1.39E+07	12.48876909
		3.00E+04	55	1.70E+06	1.65E+07	9.705882353
RSCs	B	1.00E+04	55	5.67E+05	9.56E+06	16.86067019
		2.00E+04	9.5	1.90E+05	2.30E+06	12.10526316
		3.00E+04	9.5	2.85E+05	3.20E+06	11.24210526
RSCs	C	1.00E+04	55	5.67E+05	7.96E+06	14.03880071
		2.00E+04	9.5	1.90E+05	1.88E+06	9.873684211
		3.00E+04	9.5	2.85E+05	3.32E+06	11.66315789

Table 6.5 - **Shapiro-Wilk and Levene's test results of cell number fold increase data (Table 6.4)** to test for data normality and homoscedasticity, respectively. Shapiro-Wilk test null hypothesis (H0): the data is normally distributed; Levene's test null hypothesis (H0): the groups variances are equal. Alpha = 0.05. Reject H0 if significance (p-value) < 0.05. Degrees of freedom (Df).

	Seeding density (cells per cm^2)	Shapiro-Wilk test			Levene's test			
		Statistic	Df	Significance	Statistic	Df1	Df2	Significance
Cell number fold increase (ESCs)	1.00E+04	0.806	3	0.128	0.317	2	6	0.74
	2.00E+04	0.999	3	0.954				
	3.00E+04	0.842	3	0.220				
Cell number fold increase (RSCs)	1.00E+04	0.882	3	0.331	0.938	2	6	0.427
	2.00E+04	0.857	3	0.260				
	3.00E+04	0.902	3	0.393				

Table 6.6 - **One-way ANOVA test results of cell number fold increase (Table 6.4) to detect significant diferences between ESCs and between RSCs**. One-way ANOVA null hypothesis (H0): there are no significant differences in cell number ratio between samples of this cell type. Alpha=0.05. Reject H0 if significance (p-value) < 0.05. Degrees of freedom (Df).

	One-way ANOVA		
	Statistic	Df	Significance
Cell number fold increase (ESCs)	8.801	2	0.016
Cell number fold increase (RSCs)	11.554	2	0.009

Table 6.7 - **Post-hoc Tukey test results of cell number fold increase (Table 6.4) to detect which seeding densities present significant diferences between ESCs and between RSCs.** Tukey test null hypothesis (H0): there are no significant differences in cell number ratio means between the compared seeding densities groups. Alpha=0.05. Reject H0 if significance (p-value) < 0.05.

	Seeding density (cells per cm^2)		Post-hoc Tukey test	
	Density (I)	Density (J)	Average difference (I-J)	Significance
Cell number fold increase (ESCs)	1.00E+04	2.00E+04	2.522033	0.085
		3.00E+04	-1.435861	0.354
	2.00E+04	1.00E+04	-2.522033	0.085
		3.00E+04	-3.957895	0.014
	3.00E+04	1.00E+04	1.435861	0.354
		2.00E+04	3.957895	0.014
Cell number fold increase (RSCs)	1.00E+04	2.00E+04	4.642448	0.019
		3.00E+04	5.261305	0.011
	2.00E+04	1.00E+04	-4.642448	0.019
		3.00E+04	0.618857	0.866
	3.00E+04	1.00E+04	-5.261305	0.011
		2.00E+04	-0.618857	0.866

Table 6.8 - **Levene's test (**for homoscedasticity) **and t-test results of cell number fold increase (Table 6.4) to detect significant differences between same seeding densities groups in ESCs and RSCs**. Levene's test null hypothesis (H0): the groups variances are equal; T-test null hypothesis (H0): the cell number ratio is not significantly different between the tested groups. Degrees of freedom (Df). Alpha=0.05. Reject H0 if significance (p-value) < 0.05

	Seeding density (cells per cm^2)	Levene's test		T-test		
		Statistic	Significance	Statistic	Df	Significance
Cell number fold increase ESCs-RSCs	1.00E+04	0.847	0.409	4.124	4	0.015
	2.00E+04	0.808	0.411	7.41	4	0.002
	3.00E+04	0.223	0.661	13.002	4	0

Table 6.9 - **Nanodrop RNA measurements for samples collected at Day 7, 10 and 13 of 2D Primitive endoderm differentiation assay and ESCs/RSCs controls** at Day 0 in 2i or rosette medium, respectively. All samples from GATA6::GFP reporter cell line. The concentration RNA values shown represent an average of the two measurments performed for each sample.

Sample	Cell type	Cell density per cm2	RNA (ng/µL)	1 µg RNA (µL)
PrE differentiation Day 7	ESCs	1.00E+04	287.9	3.47
		2.00E+04	621.55	1.61
		3.00E+04	628.25	1.59
	RSCs	1.00E+04	192	5.21
		2.00E+04	180.85	5.53
		3.00E+04	369.3	2.71
PrE differentiation Day 10	ESCs	1.00E+04	566.5	1.77
		2.00E+04	829.35	1.21
		3.00E+04	870.35	1.15
	RSCs	1.00E+04	163.1	6.13
		2.00E+04	278.35	3.6
		3.00E+04	705.2	1.42
PrE differentiation Day 13	ESCs	1.00E+04	1051.2	0.95
		2.00E+04	1359.3	0.74
		3.00E+04	247.65	4.05
	RSCs	1.00E+04	1329.6	0.75
		2.00E+04	96.2	10.4
		3.00E+04	1336.35	0.75
Control (in 2i) Day 0	ESCs	3.13E+04	796.6	1.26
Control Day 0	RSCs	4.16E+04	1057.15	0.95

Table 6.10 – **Normalized expression against housekeeping gene (Gapdh) of primitive endoderm markers Sox17, Gata4, Pdgfrα and naïve pluripotency marker Nanog in control samples (Day 0 ESCs and RSCs) and 2D Primitive endoderm differentiation assay samples**. All timepoints and initial cell seeding densities for both replicates (A and B). Missing values represent samples for which RNA collection was not possible. N.D. stands for expression not detected upon qPCR run.

Sample		Gene	Normalized Gene Expression					
			A			B		
Day 0 (Control)	ESCs	Sox17	9.24E-08			1.53E-07		
		Gata4	2.02E-04			7.53E-05		
		Nanog	6.80E-02			1.64E-01		
		Pdgfrα	1.75E-05			1.45E-05		
	RSCs	Sox17	5.70E-08			1.05E-07		
		Gata4	1.47E-05			3.63E-04		
		Nanog	1.12E-01			9.91E-02		
		Pdgfrα	1.26E-05			1.36E-05		
			1E+04 cells per cm^2		2E+04 cells per cm^2		3E+04 cells per cm^2	
			A	B	A	B	A	B
Day 7	ESCs	Sox17	2.08E-06	2.23E-06	1.03E-06	1.90E-06	7.26E-07	3.45E-06
		Gata4	3.94E-03	8.06E-03	1.92E-03	6.33E-03	5.29E-04	6.74E-03
		Nanog	4.12E-02	2.66E-02	4.26E-02	4.22E-02	5.49E-02	5.35E-02
		Pdgfrα	1.15E-04	5.28E-05	6.51E-05	4.25E-05	6.27E-05	5.49E-05
	RSCs	Sox17	N.D.	9.49E-07	N.D.		N.D.	
		Gata4	2.89E-04	7.29E-04	2.10E-04		1.49E+01	
		Nanog	1.95E-02	1.20E-02	3.93E-02		4.30E-01	
		Pdgfrα	1.35E-04	4.76E-05	5.11E-05		4.27E+00	
Day 10	ESCs	Sox17	4.87E-06	8.10E-06	5.23E-06	6.55E-06	1.61E-06	9.31E-06
		Gata4	2.29E-03	4.40E-03	1.80E-03	3.75E-03	6.48E-04	3.79E-03
		Nanog	3.64E-02	2.40E-02	5.38E-02	2.23E-02	4.46E-02	2.62E-02
		Pdgfrα	4.34E-05	4.47E-05	3.43E-05	4.31E-05	2.22E-05	5.10E-05
	RSCs	Sox17	6.15E-07	6.81E-07	6.20E-07		5.11E-07	3.54E-07
		Gata4	3.91E-04	1.31E-03	5.21E-04		2.90E-04	2.96E-04
		Nanog	4.57E-02	1.70E-02	4.70E-02		5.04E-02	1.40E-02
		Pdgfrα	4.17E-05	1.40E-05	3.59E-05		2.73E-05	1.91E-05
Day 13	ESCs	Sox17	2.51E-05	2.38E-05	9.38E-06	9.53E-06	1.37E-06	2.19E-05
		Gata4	7.25E-03	1.26E-02	3.01E-03	9.57E-03	1.02E-03	1.22E-02
		Nanog	5.29E-02	2.46E-02	5.69E-02	2.30E-02	3.30E-02	3.00E-02
		Pdgfrα	1.33E-04	1.45E-04	6.63E-05	1.40E-04	4.33E-05	1.76E-04
	RSCs	Sox17	1.40E-06		2.98E-06	6.06E-07	7.70E-07	7.57E-07
		Gata4	9.69E-04		8.39E-04	5.33E-04	5.43E-04	7.22E-04
		Nanog	6.42E-02		5.98E-02	3.92E-02	5.31E-02	2.17E-02
		Pdgfrα	3.39E-05		2.54E-05	6.19E-05	2.59E-05	7.25E-05

Table 6.11 - **2D Primitive endoderm differentiation assay samples' gene expression ratio against day 0 (gene expression day X / gene expression day 0) for primitive endoderm markers Sox17, Gata4, Pdgfrα and naïve pluripotency marker Nanog**. Based on normalized gene expression values from Table 6.10. Discrimination of all samples by initial cell seeding density and timepoint (day 7, 10 and 13). Values for both replicates (A and B) presented. Missing values represent samples for which RNA collection was not possible. N.D. stands for expression not detected upon qPCR run.

Sample		Gene	Gene Expression against Day 0					
			1E+04 cells per cm^2		2E+04 cells per cm^2		3E+04 cells per cm^2	
			A	B	A	B	A	B
Day 7	ESCs	Sox17	22.553	14.602	11.198	12.434	7.863	22.540
		Gata4	19.477	106.987	9.501	83.971	2.614	89.400
		Nanog	0.606	0.162	0.628	0.257	0.808	0.327
		Pdgfrα	6.582	3.632	3.720	2.920	3.581	3.778
	RSCs	Sox17	N.D.	9.033	N.D.		N.D.	
		Gata4	19.678	2.007	14.308		14.872	
		Nanog	0.175	0.121	0.351		0.430	
		Pdgfrα	10.706	3.491	4.064		4.274	
Day 10	ESCs	Sox17	52.753	52.949	56.592	42.839	17.414	60.885
		Gata4	11.337	58.461	8.904	49.769	3.204	50.294
		Nanog	0.536	0.146	0.792	0.136	0.656	0.160
		Pdgfrα	2.476	3.076	1.961	2.965	1.266	3.506
	RSCs	Sox17	10.794	6.489	10.887		8.974	3.374
		Gata4	26.624	3.599	35.492		19.735	0.816
		Nanog	0.409	0.172	0.420		0.450	0.141
		Pdgfrα	3.319	1.028	2.860		2.177	1.398
Day 13	ESCs	Sox17	271.595	155.666	56.592	62.303	14.806	143.430
		Gata4	35.834	167.507	8.904	127.002	5.036	161.815
		Nanog	0.778	0.150	0.792	0.140	0.486	0.183
		Pdgfrα	7.614	9.943	1.961	9.650	2.470	12.129
	RSCs	Sox17	24.638		52.267	5.769	13.507	7.211
		Gata4	66.024		57.170	1.467	36.989	1.990
		Nanog	0.575		0.535	0.396	0.475	0.219
		Pdgfrα	2.699		2.020	4.540	2.065	5.318

Table 6.12 - **Results for embryoid bodies model for Primitive endoderm differentiation, at 72h. Total count of embryoid bodies regarding EBs Gata6::GFP expression and morphology for all conditions**. Morphology classified in a dual system of round or random. All experimental replicates represented. Retinoic acid (R.A).

Conditions	72h			Replicate		
				A	B	C
ESC	EB morphology	Rounded	GFP Positive	359	259	312
			GFP Negative	60	93	40
		Random	GFP Positive	1	1	2
			GFP Negative	10	42	43
	Total			430	395	397
RSC	EB morphology	Rounded	GFP Positive	62	14	33
			GFP Negative	61	71	32
		Random	GFP Positive	9	7	14
			GFP Negative	290	338	343
	Total			422	430	422
ESC - R.A	EB morphology	Rounded	GFP Positive	0	0	0
			GFP Negative	429	386	429
		Random	GFP Positive	0	0	0
			GFP Negative	1	1	1
	Total			430	387	430
RSC - R.A	EB morphology	Rounded	GFP Positive	0	0	0
			GFP Negative	405	296	390
		Random	GFP Positive	0	0	0
			GFP Negative	10	15	40
	Total			415	311	430
ESC - LIF	EB morphology	Rounded	GFP Positive	343	216	250
			GFP Negative	46	105	32
		Random	GFP Positive	12	11	29
			GFP Negative	29	80	100
	Total			430	412	411
RSC - LIF	EB morphology	Rounded	GFP Positive	42	22	15
			GFP Negative	41	18	9
		Random	GFP Positive	14	9	6
			GFP Negative	330	351	400
	Total			427	400	430
RSC (48h in 2i)	EB morphology	Rounded	GFP Positive	257	151	225
			GFP Negative	152	227	143
		Random	GFP Positive	4	2	15
			GFP Negative	17	45	47
	Total			430	425	430

Table 6.13 – **Results for embryoid bodies model for Primitive endoderm differentiation, at 96h. Total count of embryoid bodies regarding EBs Gata6::GFP expression and morphology for all conditions**. Morphology classified in a dual system of round or random. All experimental replicates represented. Retinoic acid (R.A).

Conditions	96h			Replicate		
				A	B	C
ESC	EB morphology	Rounded	GFP Positive	372	276	314
			GFP Negative	47	76	38
		Random	GFP Positive	1	13	2
			GFP Negative	10	30	43
	Total			430	395	397
RSC	EB morphology	Rounded	GFP Positive	64	39	40
			GFP Negative	59	46	25
		Random	GFP Positive	9	9	14
			GFP Negative	290	336	343
	Total			422	430	422
ESC - R.A	EB morphology	Rounded	GFP Positive	0	0	0
			GFP Negative	429	386	429
		Random	GFP Positive	0	0	0
			GFP Negative	1	1	1
	Total			430	387	430
RSC - R.A	EB morphology	Rounded	GFP Positive	0	0	0
			GFP Negative	405	296	384
		Random	GFP Positive	0	0	0
			GFP Negative	10	15	46
	Total			415	311	430
ESC - LIF	EB morphology	Rounded	GFP Positive	351	252	250
			GFP Negative	38	69	32
		Random	GFP Positive	12	17	29
			GFP Negative	29	74	100
	Total			430	412	411
RSC - LIF	EB morphology	Rounded	GFP Positive	52	22	15
			GFP Negative	31	18	9
		Random	GFP Positive	14	13	6
			GFP Negative	330	347	400
	Total			427	400	430
RSC (48h in 2i)	EB morphology	Rounded	GFP Positive	268	180	256
			GFP Negative	141	198	112
		Random	GFP Positive	4	2	15
			GFP Negative	17	45	47
	Total			430	425	430

Table 6.14 - **Results for the embryoid bodies model for Primitive endoderm differentiation, at 96h. Total count of live and dead EBs, for all conditions**. Viability of cells assessed with Hoechst staining. All experimental replicates represented. Retinoic acid (R.A).

Conditions	EBs	Replicate		
		A	B	C
ESC	Live	388	353	323
	Dead	42	42	74
RSC	Live	280	288	212
	Dead	142	142	210
ESC - R.A	Live	426	383	430
	Dead	4	4	0
RSC - R.A	Live	405	301	423
	Dead	10	10	7
ESC - LIF	Live	351	333	335
	Dead	79	79	76
RSC - LIF	Live	281	281	303
	Dead	146	119	127
RSC (48h in 2i)	Live	359	354	378
	Dead	71	71	52

Table 6.15 - **Results for embryoid bodies model for Primitive endoderm differentiation. Percentage of Gata6::GFP positive EBs from the total number of EBs at 72h and 96h, in all conditions**. All experimental replicates represented. Retinoic acid (R.A).

Conditions	Replicates	EBs GFP +	
		72h	96h
ESC	A	83.72%	86.74%
	B	65.82%	73.16%
	C	79.09%	79.60%
RSC	A	16.82%	17.30%
	B	4.88%	11.16%
	C	11.14%	12.80%
ESC - R.A	A	0.00%	0.00%
	B	0.00%	0.00%
	C	0.00%	0.00%
RSC - R.A	A	0.00%	0.00%
	B	0.00%	0.00%
	C	0.00%	0.00%
ESC - LIF	A	82.56%	84.42%
	B	59.48%	65.29%
	C	67.88%	67.88%
RSC - LIF	A	13.11%	15.46%
	B	7.75%	8.75%
	C	4.88%	4.88%
RSC (48h in 2i)	A	60.70%	63.26%
	B	36.00%	42.82%
	C	55.81%	63.02%

Table 6.16 - **Shapiro-Wilk test results for EBs GFP Positive data at 72h and 96h** (Table 6.15) to test for data normality. Shapiro-Wilk test null hypothesis (H0): the data is normally distributed. Alpha = 0.05. Reject H0 if significance (p-value) < 0.05. Degrees of freedom (Df). Blank values not calculated due to equal values for all replicates.

	Condition	Shapiro-Wilk test		
		Statistic	Df	Significance
EBs GFP + 72h	ESC	0.928	3	0.481
	ESC -LIF	0.976	3	0.703
	ESC -R.A		3	
	RSC	0.999	3	0.948
	RSC -LIF	0.970	3	0.669
	RSC -R.A		3	
	RSC (48h in 2i)	0.891	3	0.359
EBs GFP + 96h	ESC	0.999	3	0.942
	ESC -LIF	0.850	3	0.239
	ESC -R.A		3	
	RSC	0.932	3	0.496
	RSC -LIF	0.977	3	0.706
	RSC -R.A		3	
	RSC (48h in 2i)	0.759	3	0.019

Table 6.17 - **Levene's test (**for homoscedasticity) **and U-Mann Whitney test** (non-parametric) **or t-test** (parametric) **results to detect significant differences between EBs GFP Positive data at 72h and 96h** (Table 6.15). Parametric and non-parametric tests performed according to fulfilled assumptions for data normality (Table 6.16) and homoscedasticity assumptions. Levene's test null hypothesis (H0): the groups variances are equal; U Mann-Whitney /T-test null hypothesis (H0): the percentage of EBs GFP Positive at 72h and 96h in the tested condition is not significantly different. Degrees of freedom (Df). Alpha=0.05. Reject H0 if significance (p-value) < 0.05. Levene's test was not calculated for RSC (48h in 2i) due to lack of data normality (Table 6.16). *Could not be calculated due to standard deviation being equal to zero.

Category	Conditions compared	Levene's test		T-test			U Mann-Whitney test	
	72h 96h	Statistic	Significance	Statistic	Df	Significance	Statistic	Significance
EBs GFP +	ESC	0.563	0.495	-0.545	4	0.615		
	ESC -LIF	0.079	0.793	-0.704	4	0.52		
	ESC -R.A	*						
	RSC	0.767	0.431	-0.767	4	0.486		
	RSC -LIF	0.196	0.681	-0.284	4	0.79		
	RSC -R.A	*						
	RSC (48h in 2i)						2	0.4

Table 6.18 - **Shapiro-Wilk and Levene's test results (**for data normality and homoscedasticity, respectively**) for embryoid bodies model for Primitive endoderm differentiation, at 96h for all conditions** (Table 3.1), **for: embryoid bodies (EB) with round morphology, EBs Gata6::GFP Positive (GFP+), EBs GFP+ with a round morphology, increase of EBs GFP+ from 72h to 96h and live EBs**. Shapiro-Wilk test null hypothesis (H0): the data is normally distributed; Levene's test null hypotheis (H0): the groups variances are equal. Alpha = 0.05. Reject H0 if significance (p-value) < 0.05. Degrees of freedom (Df). Retinoic acid (R.A). Blank values in Shapiro-Wilk test not calculated due to equal values for all replicates.

Category	Condition	Shapiro-Wilk test			Levene's test			
		Statistic	Df	Significance	Statistic	Df1	Df2	Significance
EBs round morphology	ESC	0.788	3	0.087	3.710	2	6	0.089
	ESC -LIF	0.993	3	0.836				
	ESC -R.A	0.817	3	0.156				
	RSC	0.958	3	0.603	-			
	RSC -LIF	0.767	3	0.039				
	RSC -R.A	0.945	3	0.548				
	RSC (48h in 2i)	0.972	3	0.678				
EBs GFP+	ESC	0.999	3	0.942	5.132	2	6	0.050
	ESC -LIF	0.850	3	0.239				
	ESC -R.A	-	3	-				
	RSC	0.932	3	0.496	-			
	RSC -LIF	0.977	3	0.710				
	RSC -R.A	-	3	-				
	RSC (48h in 2i)	0.759	3	0.019				
EBs GFP+ round morphology	ESC	0.814	3	0.149	3.637	2	6	0.092
	ESC -LIF	0.993	3	0.835				
	ESC -R.A	-	3	-				
	RSC	0.999	3	0.939	-			
	RSC -LIF	0.998	3	0.916				
	RSC -R.A	-	3	-				
	RSC (48h in 2i)	0.812	3	0.144				
% GFP increase 72h vs 96h	ESC	0.977	3	0.712	3.659	2	6	0.091
	ESC -LIF	0.959	3	0.609				
	ESC -R.A	-	3	-				
	RSC	0.895	3	0.371	-			
	RSC -LIF	0.994	3	0.857				
	RSC -R.A	-	3	-				
	RSC (48h in 2i)	0.812	3	0.143				
% live EBs	ESC	0.822	3	0.169	11.791	2	6	0.008
	ESC -LIF	0.859	3	0.264				
	ESC -R.A	0.824	3	0.174				
	RSC	0.778	3	0.063	-			
	RSC -LIF	0.785	3	0.078				
	RSC -R.A	1.000	3	0.983				
	RSC (48h in 2i)	0.782	3	0.071				

Table 6.19 - **Cell count results for treatments with iMyc and imTOR inhibitors, and control, for both ESCs and RSCs from R1 cell line**. Initial cell count was corrected for volume of trypsin+EDTA used for each condition. The cell number fold increase was calculated by dividing the volume corrected cell count with the nª of initial cells plated. Plating density

Initial cells plated	Condition	Cell line	Replicate	Cell count per mL	Volume corrected Cell Count	Cell number fold increase
1.20E+05	ESC	R1	1	8.5E+05	2.1E+05	1.767
			2	8.6E+05	2.2E+05	1.792
			3	8.8E+05	2.2E+05	1.823
	ESC+iMyc	R1	1	3.2E+05	8.0E+04	0.665
			2	3.7E+05	9.3E+04	0.771
			3	3.8E+05	9.5E+04	0.792
	ESC+imTOR	R1	1	2.9E+05	7.3E+04	0.606
			2	2.3E+05	5.9E+04	0.488
			3	3.1E+05	7.8E+04	0.648
1.60E+05	RSC	R1	1	8.9E+05	2.2E+05	1.389
			2	9.0E+05	2.2E+05	1.398
			3	8.9E+05	2.2E+05	1.388
3.50E+05	RSC+iMyc	R1	1	2.3E+05	9.1E+04	0.261
			2	2.4E+05	9.6E+04	0.275
			3	3.0E+05	1.2E+05	0.342
	RSC+imTOR	R1	1	2.0E+05	8.0E+04	0.227
			2	1.4E+05	5.5E+04	0.157
			3	2.1E+05	8.3E+04	0.238

Table 6.20 - **Cell count results for treatments with Myc and mTOR inhibitors, and control, for both ESCs and RSCs from IB10 cell line**. Initial cell count was corrected for volume of trypsin+EDTA used for each condition. The cell number fold increase was calculated by dividing the volume corrected cell count with the nº of initial cells plated. Plating density was maintained in all conditions in each cell type.

Initial cells plated	Condition	Cell line	Replicate	Cell count per mL	Volume corrected Cell Count	Cell number fold increase
1.20E+05	ESC	IB10	1	8.57E+05	2.14E+05	1.785
			2	8.80E+05	2.20E+05	1.833
			3	8.20E+05	2.05E+05	1.708
	ESC+iMyc	IB10	1	3.26E+05	8.15E+04	0.679
			2	3.91E+05	9.78E+04	0.815
			3	3.87E+05	9.68E+04	0.806
	ESC+imTOR	IB10	1	3.10E+05	7.75E+04	0.646
			2	2.84E+05	7.10E+04	0.592
			3	3.16E+05	7.90E+04	0.658
1.60E+05	RSC	IB10	1	9.17E+05	2.29E+05	1.433
			2	9.02E+05	2.26E+05	1.409
			3	8.75E+05	2.19E+05	1.367
3.50E+05	RSC+iMyc	IB10	1	2.39E+05	9.56E+04	0.273
			2	2.76E+05	1.10E+05	0.316
			3	2.40E+05	9.60E+04	0.274
	RSC+imTOR	IB10	1	2.15E+05	8.60E+04	0.246
			2	1.93E+05	7.71E+04	0.220
			3	2.11E+05	8.44E+04	0.241

Table 6.21 - **Cell number fold increase for all conditions in embryonic diapause experiment** (ESC, RSC, ESC/RSC with Myc inhibitor, ESC/RSC with mTOR inhibitor) **normalized against respective controls** (ESC for ESC+iMyc and ESC+imTOR, RSC for RSC+iMyc and RSC+imTOR)**.** The variation from initial cell number was calculated by dividing the volume corrected cell count with the nº of initial cells plated. All three replicates from R1 and IB10 cell lines are represented.

	Condition	Replicate	Cell line	
			R1	IB10
Normalized cell number fold increase	ESC	1	1	1
		2	1	1
		3	1	1
	ESC+iMyc	1	0.38	0.380397
		2	0.43	0.444318
		3	0.43	0.471951
	ESC+imTOR	1	0.34	0.361727
		2	0.27	0.322727
		3	0.36	0.385366
	RSC	1	1	1
		2	1	1
		3	1	1
	RSC+iMyc	1	0.19	0.190634
		2	0.2	0.22397
		3	0.25	0.20062
	RSC+imTOR	1	0.16	0.171491
		2	0.11	0.156341
		3	0.17	0.176379

Table 6.22 - **Levene's test** (for homoscedasticity) **and t-test results to detect significant differences normalized cell number fold increase between same conditions from R1 and IB10 cell lines** (Table 6.21). Levene's test null hypothesis (H0): the groups variances are equal. T-test null hypothesis (H0): the normalized variation from initial cell number in the tested conditions is not significantly different. Degrees of freedom (Df). Alpha=0.05. Reject H0 if significance (p-value) < 0.05.

	Cell line	Conditions compared	Levene's test		T-test		
			Statistic	Significance	Statistic	Df	Significance
Normalized Cell number fold increase	R1 vs. IB10	ESC+iMyc	0.519	0.511	0.566	4	0.602
		ESC+imTOR	0.835	0.412	-1.041	4	0.357
		RSC+iMyc	2.17	0.215	0.243	4	0.82
		RSC+imTOR	5.843	0.073	-0.973	4	0.418

Table 6.23 - **Shapiro-Wilk test results for normalized cell number fold increase, embryonic diapause experiment (Table 6.21)** to test for data normality. Shapiro-Wilk test null hypothesis (H0): the data is normally distributed. Alpha = 0.05. Reject H0 if significance (p-value) < 0.05. Degrees of freedom (Df). *not calculated, values equal for all replicates

	Cell line	Condition	Shapiro-Wilk test		
			Statistic	Df	Significance
Normalized Cell number fold increase	R1	ESC	*	3	*
		ESC+imTOR	0.858	3	0.261
		ESC+iMyc	0.802	3	0.119
		RSC	*	3	*
		RSC+imTOR	0.844	3	0.225
		RSC+iMyc	0.860	3	0.269
	IB10	ESC	*	3	*
		ESC+imTOR	0.980	3	0.731
		ESC+iMyc	0.950	3	0.570
		RSC	*	3	*
		RSC+imTOR	0.920	3	0.451
		RSC+iMyc	0.949	3	0.566

Table 6.24 - **Levene's test** (for homoscedasticity) **and t-test results to detect significant differences in normalized cell number fold increase between the conditions with Myc and mTOR inhibitors for embryonic diapause experiment** (Table 6.21). Levene's test null hypothesis (H0): the groups variances are equal. T-test null hypothesis (H0): the normalized variation from initial cell number in the tested conditions is not significantly different. Degrees of freedom (Df). Alpha=0.05. Reject H0 if significance (p-value) < 0.05.

	Conditions compared	Cell line	Levene's test		T-test		
			Statistic	Significance	Statistic	Df	Significance
Normalized Cell number fold increase	ESC+iMyc	R1	0.008	0.933	7.777	4	0.001
	RSC+iMyc	IB10	3.08	0.154	7.872	4	0.001
	ESC+imTOR	R1	0.717	0.445	5.458	4	0.005
	RSC+imTOR	IB10	2.588	0.183	9.803	4	0.001
	ESC+iMyc	R1	0.698	0.451	2.81	4	0.048
	ESC+imTOR	IB10	0.661	0.462	2.313	4	0.082
	RSC+iMyc	R1	0.004	0.953	2.341	4	0.079
	RSC+imTOR	IB10	0.949	0.385	3.197	4	0.033

Table 6.25 – **Number of colonies (pluripotent and not pluripotent) after ESCs and RSCs recovery period from treatment with Myc and mTOR inhibitors.** Colonies fixed, stained with alkaline-phosphatase and counted 72h after plating ESCs and RSCs from iMyc, imTOR and control conditions in 2i media, at clonal density **(**400 cells for a single 24-well).

Conditions (all in 2i)	Cell line	Number of colonies	
		Pluripotent	Not pluripotent
ESC	R1	262	0
	IB10	286	0
ESC+iMyc	R1	163	0
	IB10	222	0
ESC+imTOR	R1	144	3
	IB10	127	0
RSC	R1	218	0
	IB10	224	0
RSC+iMyc	R1	141	0
	IB10	172	0
RSC+imTOR	R1	101	0
	IB10	69	0

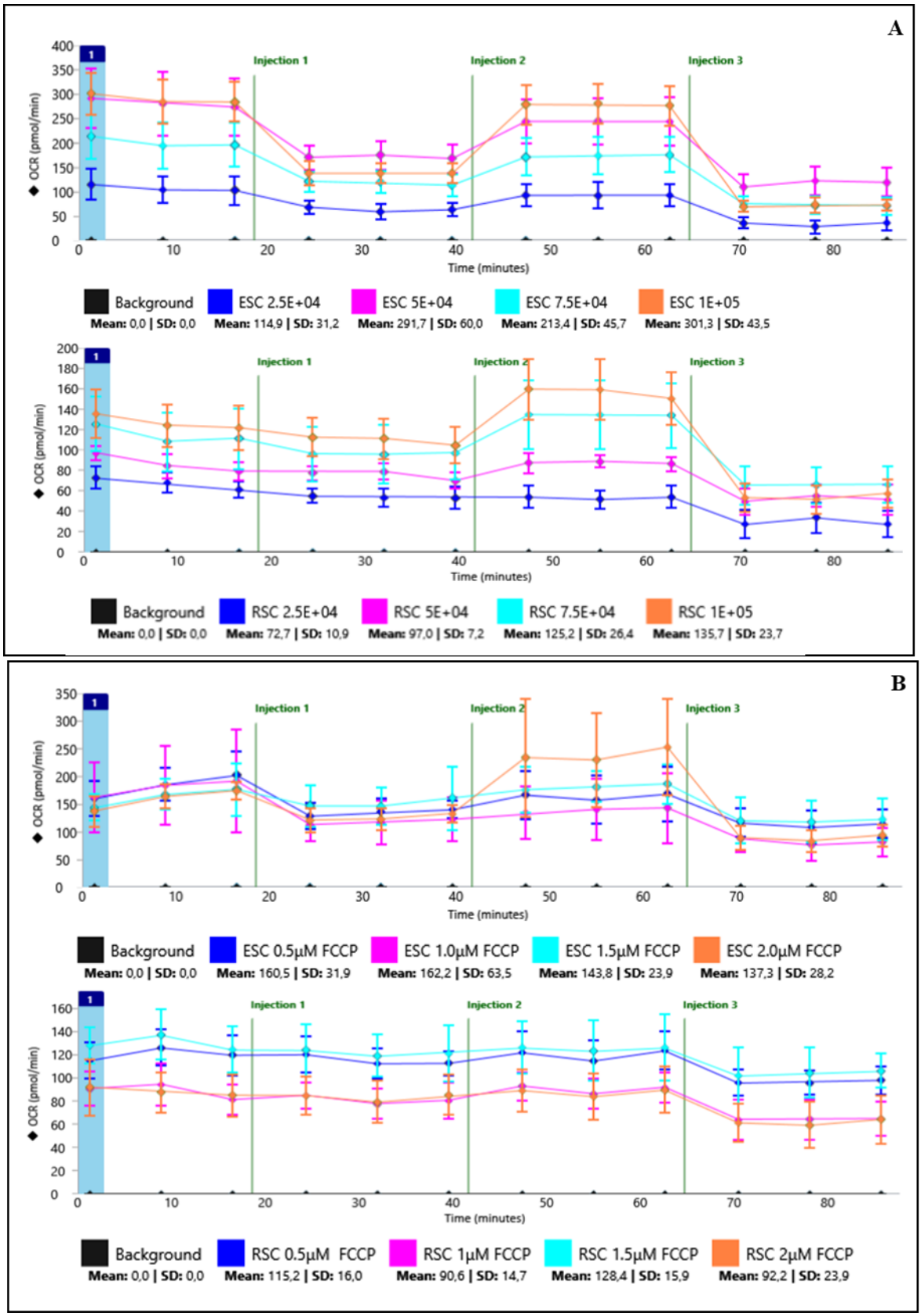

Figure 6.1 – **Seahorse Extracellular Flux analyzer assay (ESC -2i -and RSC) for (A) cell number and (B) FCCP concentration optimization.** Cell numbers tested: 25000, 50000, 75000 and 100000 cells; FCCP concentrations tested: 0.5 µM, 1.0 µM, 1.5 µM and 2.0 µM . Plotted OCR (oxygen consumption rate) values represent mean of five wells per each condition. Injection 1: oligomycin 1µM, Injection 2: FCCP 1µM (A) , Injection 3: antimycin 1µM. SD (standard deviation).

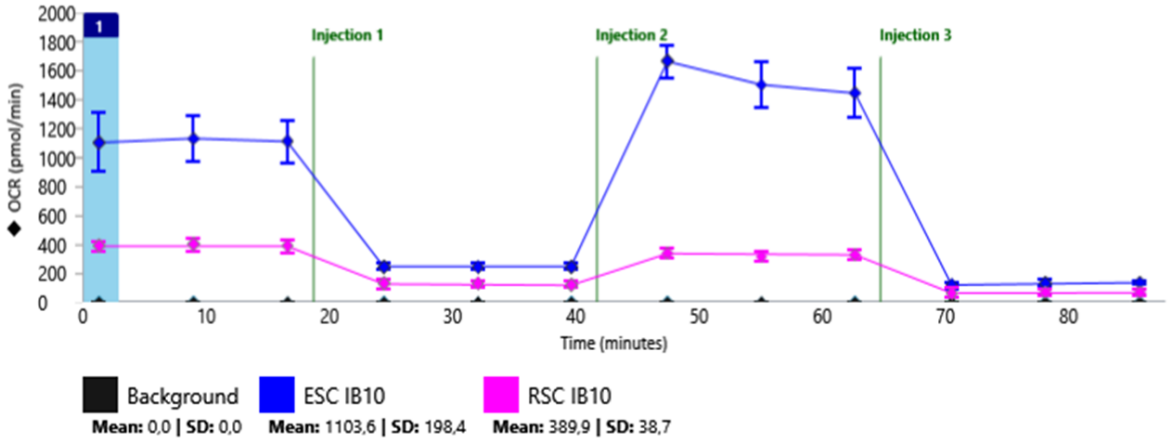

Figure 6.2 - **Seahorse Extracellular Flux analyzer assay OCR measurements for ESC and RSC, from IB10 cell line.** 1E+05 cell number in RSC, undefined density – due to experimental error – in ESCs. Plotted OCR (oxygen consumption rate) values represent mean of five wells per each density. Injection 1: oligomycin 1µM, Injection 2: FCCP 2.0 µM, , Injection 3: antimycin 1µM. SD (standard deviation).

Oxidative phosphorilation gene set		
ENSMUSG00000030653 Pde2a	ENSMUSG00000031233 Pgk2	ENSMUSG00000041881 Ndufa7
ENSMUSG00000022346 Myc	ENSMUSG00000032081 Apoc3	ENSMUSG00000025651 Uqcrc1
ENSMUSG00000046329 Slc25a23	ENSMUSG00000024248 Cox7a2l	ENSMUSG00000030717 Nupr1
ENSMUSG00000006457 Actn3	ENSMUSG00000015790 Surf1	ENSMUSG00000064358 mt-Co3
ENSMUSG00000048482 Bdnf	ENSMUSG00000031818 Cox4i1	ENSMUSG00000013593 Ndufs2
ENSMUSG00000009876 Cox4i2	ENSMUSG00000026459 Myog	ENSMUSG00000064370 mt-Cytb
ENSMUSG00000029432 Gbas	ENSMUSG00000031393 Mecp2	ENSMUSG00000024099 Ndufv2
ENSMUSG00000062070 Pgk1	ENSMUSG00000061518 Cox5b	ENSMUSG00000027282 Mtch2
ENSMUSG00000054362 Lexm	ENSMUSG00000009995 Taz	ENSMUSG00000021577 Sdha
ENSMUSG00000030785 Cox6a2	ENSMUSG00000039065 Fam173b	ENSMUSG00000071014 Ndufb6
ENSMUSG00000025889 Snca	ENSMUSG00000019942 Cdk1	ENSMUSG00000064345 mt-Nd2
ENSMUSG00000025825 Iscu	ENSMUSG00000022354 Ndufb9	ENSMUSG00000000563 Atp5f1
ENSMUSG00000024038 Ndufv3	ENSMUSG00000028964 Park7	ENSMUSG00000046909 Tefm
ENSMUSG00000038302 Lace1	ENSMUSG00000025428 Atp5a1	ENSMUSG00000024208 Uqcc2
ENSMUSG00000020664 Dld	ENSMUSG00000033792 Atp7a	ENSMUSG00000027305 Ndufaf1
ENSMUSG00000024401 Tnf	ENSMUSG00000038462 Uqcrfs1	ENSMUSG00000033751 Gadd45gip1
ENSMUSG00000014554 Dguok	ENSMUSG00000025403 Shmt2	ENSMUSG00000022890 Atp5j
ENSMUSG00000028756 Pink1	ENSMUSG00000022013 Dnajc15	ENSMUSG00000064363 mt-Nd4
ENSMUSG00000026895 Ndufa8	ENSMUSG00000025393 Atp5b	ENSMUSG00000024151 Msh2
ENSMUSG00000007815 Rhoa	ENSMUSG00000058076 Sdhc	ENSMUSG00000003072 Atp5d
ENSMUSG00000059363 Fxn	ENSMUSG00000034566 Atp5h	ENSMUSG00000031378 Abcd1
ENSMUSG00000065947 mt-Nd4l	ENSMUSG00000022956 Atp5o	ENSMUSG00000025204 Ndufb8
ENSMUSG00000031782 Coq9	ENSMUSG00000030652 Coq7	ENSMUSG00000021606 Ndufs6
ENSMUSG00000028452 Vcp	ENSMUSG00000043702 Pde12	ENSMUSG00000044894 Uqcrq
ENSMUSG00000041431 Ccnb1	ENSMUSG00000021868 Ppif	ENSMUSG00000017778 Cox7c
ENSMUSG00000025968 Ndufs1	ENSMUSG00000071654 Uqcc3	ENSMUSG00000064357 mt-Atp6
ENSMUSG00000037916 Ndufv1	ENSMUSG00000026260 Ndufa10	ENSMUSG00000020022 Ndufa12
ENSMUSG00000049422 Chchd10	ENSMUSG00000041697 Cox6a1	ENSMUSG00000063882 Uqcrh
ENSMUSG00000024668 Sdhaf2	ENSMUSG00000022551 Cyc1	ENSMUSG00000061118 Dnajc30
ENSMUSG00000028982 Slc25a33	ENSMUSG00000059534 Uqcr10	ENSMUSG00000000088 Cox5a
ENSMUSG00000074218 Cox7a1	ENSMUSG00000005373 Mlxipl	ENSMUSG00000000171 Sdhd
ENSMUSG00000004446 Bid	ENSMUSG00000064354 mt-Co2	ENSMUSG00000028455 Stoml2
ENSMUSG00000028527 Ak4	ENSMUSG00000059734 Ndufs8	ENSMUSG00000025781 Atp5c1
ENSMUSG00000038717 Atp5l	ENSMUSG00000032330 Cox7a2	ENSMUSG00000056436 Cyct
ENSMUSG00000030647 Ndufc2	ENSMUSG00000021520 Uqcrb	ENSMUSG00000038690 Atp5j2
ENSMUSG00000063694 Cycs		

List 6.1- **Gene set composed by all *Mus musculus* genes present in the oxidative phosphorylation subsection, from the metabolic process group (biological processes) from the GOTree platform from MGI database.**